JOURNAL OF VIROLOGY, June 2011, p. 5423–5435 Vol. 85, No. 11
0022-538X/11/$12.00 doi:10.1128/JVI.02146-10

Natural Killer Cells Recognize Friend Retrovirus-Infected Erythroid Progenitor Cells through NKG2D–RAE-1 Interactions *In Vivo*

Tatsuya Ogawa,[1,2]†§ Sachiyo Tsuji-Kawahara,[1]§ Takae Yuasa,[1] Saori Kinoshita,[1] Tomomi Chikaishi,[1,3] Shiki Takamura,[1] Haruo Matsumura,[1]‡ Tsukasa Seya,[4] Toshihiko Saga,[2] and Masaaki Miyazawa[1]*

Department of Immunology[1] and Department of Cardiovascular Surgery,[2] Kinki University School of Medicine, Osaka-Sayama, Osaka, Japan; Unmet Medical Needs Pharma, Inc., Yokohama, Japan[3]; and Department of Microbiology and Immunology, Hokkaido University Graduate School of Medicine, Kita-ku, Sapporo 060-8638, Japan[4]

Received 12 October 2010/Accepted 10 March 2011

Natural killer (NK) cells function as early effector cells in the innate immune defense against viral infections and also participate in the regulation of normal and malignant hematopoiesis. NK cell activities have been associated with early clearance of viremia in experimental simian immunodeficiency virus and clinical human immunodeficiency virus type 1 (HIV-1) infections. We have previously shown that NK cells function as major cytotoxic effector cells in vaccine-induced immune protection against Friend virus (FV)-induced leukemia, and NK cell depletion totally abrogates the above protective immunity. However, how NK cells recognize retrovirus-infected cells remains largely unclear. The present study demonstrates a correlation between the expression of the products of retinoic acid early transcript-1 (RAE-1) genes in target cells and their susceptibility to killing by NK cells isolated from FV-infected animals. This killing was abrogated by antibodies blocking the NKG2D receptor *in vitro*. Further, the expression of RAE-1 proteins on erythroblast surfaces increased early after FV inoculation, and administration of an RAE-1-blocking antibody resulted in increased spleen infectious centers and exaggerated pathology, indicating that FV-infected erythroid cells are recognized by NK cells mainly through the NKG2D–RAE-1 interactions *in vivo*. Enhanced retroviral replication due to host gene-targeting resulted in markedly increased RAE-1 expression in the absence of massive erythroid cell proliferation, indicating a direct role of retroviral replication in RAE-1 upregulation.

Natural killer (NK) cells play an important role in eliminating virus-infected cells via both direct killing and antibody-dependent cell-mediated cytotoxicity mechanisms (15, 49). NK cells also control adaptive immune responses through the production of key cytokines in the early stages of viral infection. In addition, NK cells have been implicated in the growth regulation of hematopoietic cells (6, 39). Thus, viruses that infect hematopoietic cells are prime targets of NK cells. In fact, NK cells are expanded and activated during acute human immunodeficiency virus type 1 (HIV-1) infection prior to seroconversion (1), and NK cell activity parallels changes in plasma viral load both in experimental infection of rhesus macaques with a pathogenic simian immunodeficiency virus isolate (10) and in clinical HIV-1 infection (21). Increased NK cell activities in high-risk HIV-1-exposed uninfected individuals (34, 38) also indicate a possible role of NK cells in resistance against HIV-1 acquisition. Genetic analyses of large cohorts have provided compelling evidence for correlations between certain haplotypes of the killer cell immunoglobulin-like receptor (KIR) loci and slow progression to AIDS after HIV-1 seroconversion (9, 23, 24), connecting NK cell activities with restricted HIV-1 replication. NK cells are also reduced in patients with human T-lymphotropic virus type 1 (HTLV-1)-associated disorders (3), indicating possible disease progression in the absence of NK cell-mediated virus control. However, little is known about the molecular mechanisms through which retrovirus-infected cells are recognized by NK cells.

Friend virus (FV) is a highly leukemogenic and immunosuppressive mouse retrovirus complex composed of replication-competent Friend murine leukemia virus (F-MuLV) and replication-defective but acutely transforming Friend spleen focus-forming virus (SFFV). The product of the SFFV *env* gene, gp55, forms a complex with the erythropoietin receptor and the short form of the hematopoietic cell-specific receptor tyrosine kinase (STK), and this interaction induces the growth and terminal differentiation of erythroid progenitor cells, causing polycythemia and massive splenomegaly (18, 28). The resultant increase in targets of FV integration consequently causes the emergence of mono- or oligoclonal erythroleukemia through insertional activation of transcription factors or disruption of a tumor suppressor gene. Since the above early splenomegaly and late erythroleukemogenesis can be induced by inoculating the virus into immunocompetent adult mice of susceptible strains, FV has contributed to the analysis of host immune responses that influence retrovirus replication and disease development (5, 12, 25, 27).

We previously showed that the majority of cytotoxic effector cells detected early after FV infection were NK rather than

* Corresponding author. Mailing address: Department of Immunology, Kinki University School of Medicine, 377-2 Ohno-Higashi, Osaka-Sayama, Osaka 589-8511, Japan. Phone and fax: 81-72-367-7660. E-mail: masaaki@med.kindai.ac.jp.
§ T. Ogawa and S. Tsuji-Kawahara contributed equally to this study.
† Present address: National Cerebral and Cardiovascular Center, Suita, Osaka, Japan.
‡ Department of Basic Medical Sciences, Kinki University Faculty of Medicine, Osaka-Sayama, Osaka, Japan.
Published ahead of print on 16 March 2011.

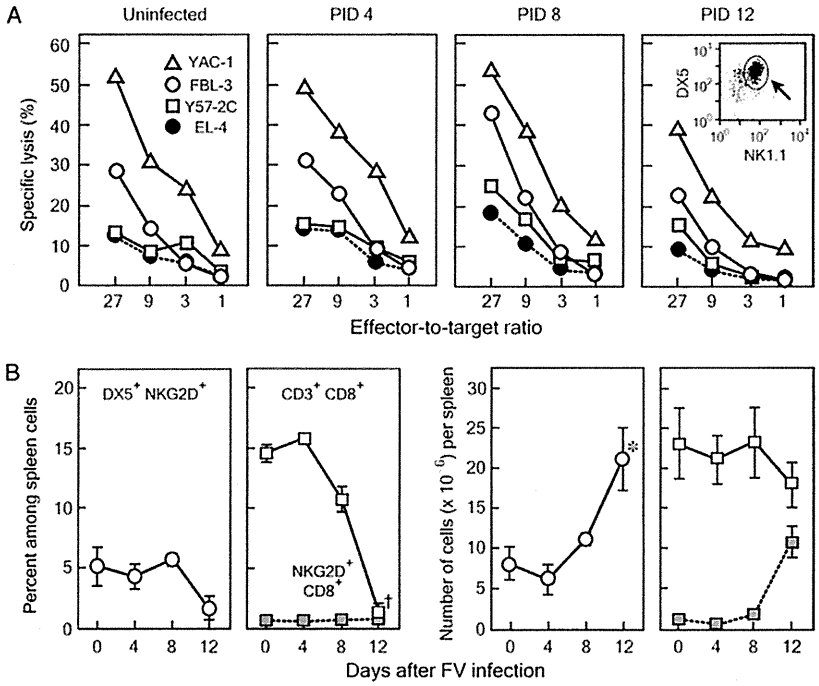

FIG. 1. Changes in NK cell activities and numbers in CB6F$_1$ mice after FV infection. (A) Killing activities of NK cells purified from CB6F$_1$ mice at various time points after FV infection on target cells of different origin. CB6F$_1$ mice were inoculated with 150 SFFU of LDV-free FV. CD4 , CD8 , B220 , and DX5 NK cells were purified from the spleens, confirmed to be 85 to 95% positive for DX5 and 76 to 86% positive for both DX5 and NK-1.1 (arrow in the inset), and used as effector cells without an *in vitro* stimulation as described previously (16). Specific lysis of 4 different lines of target cells at each indicated effector-to-target ratio was measured by ^{51}Cr release assays (16, 45). Each data point here represents a mean calculated from triplicate wells with the SEM being 10% of the average throughout the present study. Experiments were repeated 3 times with essentially the same results. (B) Percentages and absolute numbers of NK and CD8 T cells expressing NKG2D at various time points after FV infection. CB6F$_1$ mice were inoculated with FV, and spleen cells were analyzed by multicolor flow cytometry. Absolute numbers of each cell population were calculated by (total number of nucleated spleen cells percentage of the population in question)/100. Each data point here represents mean SEM calculated from 4 animals. , P 0.05 in comparison with the corresponding values at PID 0 (prior to infection) by t test; †, P 0.005.

CD8 T cells (16). Further, protective anti-FV immunity induced by a single immunization of susceptible mice with a synthetic peptide that harbored a T-helper (Th) cell epitope (26) was totally abrogated by the depletion of NK cells, without affecting the numbers and proliferative and killing functions of CD4 and CD8 T cells (16). On the other hand, mice lacking CD8 T cells were nevertheless protected against FV infection by the above immunization with the single-epitope peptide (19). Our recent study (45) has revealed rapidly induced terminal exhaustion of CD8 effector cells in FV-infected animals; thus, although activated, FV-specific CD8 T cells become unable to exert cytotoxic effector functions upon cognate binding to infected target cells by as early as 14 days after infection. These results collectively indicate that NK cells, instead of CD8 T cells, may play essential roles in controlling the proliferation of erythroid progenitor cells in acute FV infection. In fact, enhanced NK cell activities were associated with delayed development of FV-induced leukemia in mice overexpressing vascular endothelial growth factor A (VEGF-A) (4). Here we utilized the above FV model to elucidate how retrovirus-infected cells are recognized by NK cells.

MATERIALS AND METHODS

Mice and virus. C57BL/6 (B6; *Fv2*^{s} *H2*^{b}) and (BALB/c C57BL/6)F$_1$ (CB6F$_1$; *Fv2*$^{s/r}$ *H2*$^{d/b}$) mice were purchased from Japan SLC, Inc. (Hamamatsu, Japan). Breeding pairs of B6(Cg)-*Tnfrsf13c*^{tm1Mass}/J (B6-*BAFF-R* $^{-/-}$) mice homozygously carrying a targeted disruption of the receptor for B-cell activating factor belonging to the tumor necrosis factor family (*BAFF-R*) gene (37) were purchased from The Jackson Laboratory (Bar Harbor, ME). The apolipoprotein B mRNA editing enzyme catalytic polypeptide 3 (APOBEC3)-deficient mice on a B6 background (B6-*APOBEC3* $^{-/-}$) have been described previously (46, 47). Mice 8 to 12 weeks in age at the time of FV infection were used throughout the present study. The stocks of B-tropic FV without contamination of lactate dehydrogenase-elevating virus (LDV) and the infectious molecular clone of F-MuLV, FB-29, have been described previously (27, 45–47). Mice were inoculated with an indicated dose of FV or F-MuLV by intravenous injection into the tail vein. All animal experiments described here have been approved by the Animal Experiment Committee of Kinki University and performed according to the relevant laws and regulations of the Japanese government.

Purification of NK cells and cytotoxicity assays. Purification of NK cells was performed by using antibody (Ab)-conjugated micromagnetic beads as described previously (16), except that an automated magnetic cell sorting separator (autoMACS; Miltenyi Biotech GmbH, Bergisch Gladbach, Germany) was used in the present study. In brief, nucleated spleen cells in phosphate-buffered balanced salt solution (PBBS) were first mixed with a mixture of anti-mouse CD4, anti-mouse CD8, and anti-mouse B220 Ab-conjugated microbeads solution, and CD4 , CD8 , and B220 cells were depleted by using the Depletes program. The resultant CD4 , CD8 , and B220 cells were then mixed with anti-DX5 Ab-conjugated microbeads, and positive selection was performed by using the Posselds program. The resultant CD4 , CD8 , B220 , and DX5 cells were confirmed to be 85 to 95% positive for DX5 (Fig. 1A, inset) and were used as effector cells without any *in vitro* stimulation throughout the present study. The target cells used were as follows: an F-MuLV-induced leukemia cell line, FBL-3, established from a B6 mouse; a line of FV-induced leukemia cells, Y57-2C, established from a (C57BL/10 A.BY)F$_1$ (*H2*$^{b/b}$) mouse; a chemically induced

T-cell lymphoma line, EL-4, established from a B6 mouse; and an A/Sn mouse-derived Moloney murine leukemia virus (M-MuLV)-induced lymphoma line, YAC-1 (*H2*^{a}). Y57-2C cells were originally provided by Bruce Chesebro, Laboratory of Persistent Viral Diseases, NIH, NIAID, Rocky Mountain Laboratories, Hamilton, MT, and FBL-3, EL-4, and YAC-1 cells were provided by Kagemasa Kuribayashi, Mie University School of Medicine, Tsu, Japan. Cytotoxicity assays were performed by using ^{51}Cr-labeled target cells as described elsewhere (16, 45).

For the possible blocking of NK-mediated killing, low-endotoxin and azide-free functional-grade anti-mouse NKG2D Ab (clone CX5, rat IgG1 [29], and clone C7, Armenian hamster IgG [13]) were purchased from eBioscience (San Diego, CA) and added to the assay cultures at 30 g/ml according to a previously described procedure (13). Control IgG1 purified from unimmunized rat sera and monoclonal Ab A19-3 (Armenian hamster IgG) specific for trinitrophenyl hapten were purchased from eBioscience and BD Biosciences PharMingen (San Diego, CA), respectively.

Flow cytometry. Flow cytometric analyses were performed as described elsewhere (44–47). Abs used were the following: fluorescein isothiocyanate (FITC)-conjugated anti-mouse CD8 and phycoerythrin (PE)-conjugated anti-mouse NKG2D (clone CX5) (eBioscience); FITC-conjugated anti-NK1.1, biotin-conjugated anti-mouse Pan-NK (DX5), biotin-conjugated anti-mouse Qa-1^{b}, and allophycocyanin (APC)-conjugated anti-mouse TER-119 (BD Biosciences PharMingen); and PE-conjugated anti-mouse Pan–RAE-1 (R&D Systems, Inc., Minneapolis, MN). B6 mice express the alloantigen NK-1.1, and DX5 recognizes CD49b (2). TER-119 reacts with a molecule associated with glycophorin A (20) and marks late erythroblasts as well as mature red cells (50). Monoclonal Ab 720 reactive with F-MuLV gp70, but not with any other mouse retrovirus (36), was purified and conjugated with biotin as described previously (45–47). PE-conjugated (BD Biosciences PharMingen) and FITC-conjugated (DakoCytomation, Glostrup, Denmark) streptavidin were used for staining with the biotin-conjugated antibodies. All staining reactions were performed in the presence of 0.25 g/10^{6} cells of anti-mouse CD16/CD32 (BD Biosciences PharMingen). Cells were also incubated with the appropriate isotype-matched control Ab to draw demarcation lines that separate cells positively stained from those not stained. Multicolor flow cytometric analyses were performed with a Becton-Dickinson FACSCalibur and CellQuest software (BD Biosciences, Franklin Lakes, NJ).

Depletion of NK cells and blocking of NKG2D–RAE-1 interactions *in vivo*. Rabbit antiserum specific for mouse asialo ganglio-*N*-tetraosylceramide (asialo-GM1) and control normal rabbit serum were purchased from Wako Pure Chemicals (Osaka, Japan), and the IgG fraction was concentrated by precipitation with 45% (final) ammonium sulfate. Mice were injected intravenously with 60 g/dose of the anti-asialoGM1 Ab at 1 day prior to FV inoculation and 2, 5, 8, and 11 days after the virus infection as performed previously (16). For *in vivo* blocking of NKG2D, 100 g/dose anti-NKG2D Ab (CX5) or control rat IgG was administered 2 days prior to, the day of, and 2 days after FV inoculation. The lack of a detectable level of NKG2D on DX5 NK cells was confirmed 5 days after infection by flow cytometry essentially as described previously (45). Monoclonal anti-mouse RAE-1 Ab that blocks the binding of mouse NKG2D to and isoforms of mouse RAE-1 (clone 199205, rat IgG2b) (51) was purchased from R&D Systems, Inc., and 100 g/dose of this Ab or the above control rat IgG was administered the day of and 2 days after FV inoculation.

FV-induced disease development was monitored by following the survival of each representative group of infected mice for 60 days and by measuring spleen weights at 13 days after infection as described previously (16, 19). Infectious center assays were performed as described previously (19, 26). Three-fold dilutions of nucleated spleen cells between 30 and 3 10^{6}/well were prepared from each animal and were added in triplicate into a well of 24-well tissue culture plates that had been seeded with 1 10^{4} *Mus dunni* cells on the previous day. Spots of F-MuLV gp70-expressing *Mus dunni* cells in each well were counted under a magnifier after 2 days of coculturing followed by fixation and immunoenzymatic staining with monoclonal Ab 720 (36). The numbers of spleen infectious centers were calculated as averages of triplicate samples which gave close to but less than 150 spots of the infected indicator cells per well. As up to 3 10^{6} nucleated spleen cells can be seeded and up to 150 spots of infected *Mus dunni* cells can be distinguished per well, the results shown in the present study represent absolute numbers of infectious centers among 10^{5} nucleated spleen cells.

Quantitative real-time PCR assays. For the induction of NK receptor ligands, the indicated leukemia and lymphoma cells maintained in an exponential growth phase were reseeded at 2.5 10^{6} cells/5 ml/well in 6-well tissue culture plates with 5 U/ml (final) of recombinant mouse gamma interferon (IFN-) (BD Biosciences PharMingen). After the indicated hours of incubation, cells were harvested and total cellular RNA was extracted by using the TRIzol solution (Invitrogen Japan, K. K., Tokyo, Japan). Poly-A RNA was purified from total RNA for each sample by the use of the MicroFast Track 2.0 system (Invitrogen).

Quantitative real-time PCRs were performed as described previously (46, 47). The sequence-specific primers and probes used are as follows: *Raet1* forward, CGCCATCATTTTATGATTCAGAAG, reverse, TGGTCAAGTTGCACCTA AGAGAGT, and probe, 6-carboxyfluorescein (FAM)-TACTGAGCTATGGAT ACACCAACGGGCTZ-6-carboxytetramethylrhodamine (TAMRA); *Qa-1*^{b} forward, AGATCTCTAAGCACAAGTCAGAGGC, reverse, TCATTTCCCAGC CGTAGGTATC, and probe, FAM-TGAGGCCCACCAACAGAGGGCATZ-TAMRA; and F-MuLV *env* forward, GCTGCGAGACAACCGGTAGA, reverse, GCATACCTGAACAGCCTGGTTA, and probe, FAM-TTCTTGGGA CTACATCACAGTZ-TAMRA. The above primer/probe set used for the detection of the *Raet1* messages reacts with all known isoforms (-ε) of mouse *Raet1*. Specificities of the probes were confirmed by cloning and sequencing the amplified cDNA fragments as described previously (46). TaqMan rodent *GAPDH* control (Applied Biosystems, Foster City, CA) was added to each reaction mixture as a normalizer. The levels of expression of each gene tested were expressed by the threshold cycle (2 ^{CT}), where an average value and SEM were calculated for each sample.

Statistical analyses. Two-way analysis of variance (ANOVA) with Bonferroni *post hoc* tests and Mantel-Cox tests of survival curves were performed by using Prism software (GraphPad Software, Inc., San Diego, CA). Average values were compared by Student's or Welch's *t* test, depending on whether the variances of the compared samples were estimated to be equal or not, and Bonferroni's correction was applied for multiple comparisons when required. Paired *t* tests were performed when two parameters within a single experimental group were compared.

RESULTS

Changes in NK cell activities upon FV infection of susceptible mice. Mice possessing at least a single dominant *Fv2*^{s} allele develop polycythemia and splenomegaly early after FV inoculation. CB6F$_1$ mice are highly susceptible to FV and develop massive splenomegaly within 2 weeks after infection, and all die within 60 days upon inoculation, with as low as 15 spleen focus-forming units (SFFU) of FV (16, 19, 26, 27). NK cell activities were previously demonstrated with the spleens of CB6F$_1$ mice at 7 to 11 days after FV infection (16); however, the *in vivo*-passaged FV stocks used in the above and other experiments performed prior to 2007 had been contaminated unintentionally with LDV, which is known to activate NK cells soon after inoculation (27). It is possible, therefore, that the previously detected NK cell activities were evoked by LDV, rather than by FV infection. Thus, we first tested the killing activities exerted by NK cells purified from CB6F$_1$ mice at various time points after infection with LDV-free FV.

High-level killing activities were detectable against YAC-1 target cells even before FV inoculation of CB6F$_1$ mice. Killing activities against F-MuLV-induced FBL-3 tumor cells were also detected prior to FV infection, increased following FV infection, and peaked at postinoculation day (PID) 8 (Fig. 1A). Both activities, however, decreased at PID 12. The above kinetics were essentially not different from those observed by inoculating the same strain of mice with an LDV-contaminated stock of FV (data not shown). Thus, FV infection without LDV contamination enhanced constitutively detectable NK-mediated killing activities against F-MuLV-induced FBL-3 leukemia cells in CB6F$_1$ mice.

Different levels of NK-receptor ligand expression in correlation with susceptibility to NK-mediated lysis among retrovirus-induced leukemia cell lines. In the previously (16) and the above-described (Fig. 1A) experiments, the FV-induced leukemia line Y57-2C cells were almost as resistant to NK-mediated killing as EL-4 lymphoma cells were, while F-MuLV-

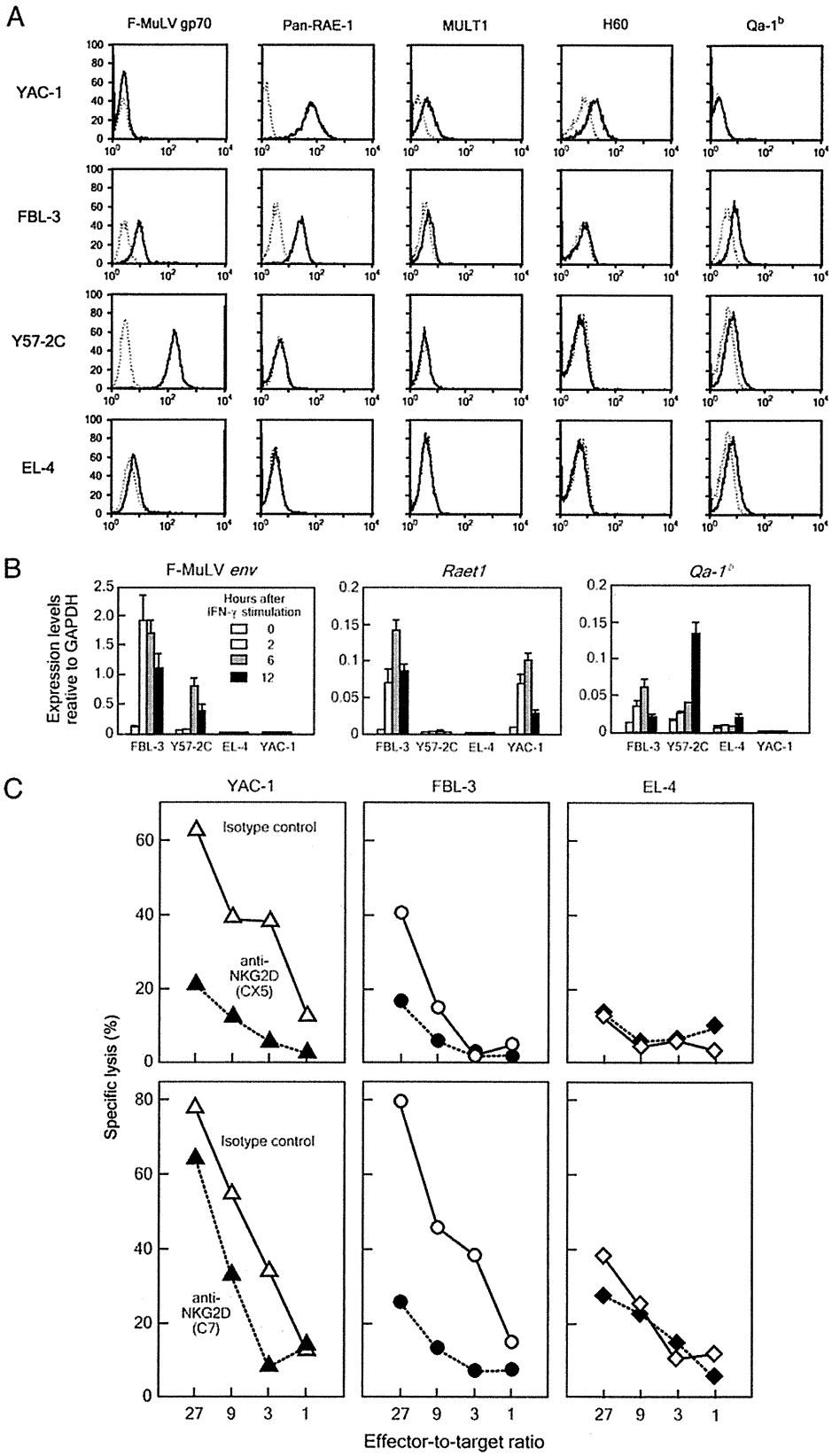

induced FBL-3 leukemia cells were killed almost as efficiently as positive control YAC-1 cells by NK cells purified from FV-infected mice at around PID 8. The above different susceptibilities to NK killing between FBL-3 and Y57-2C cells were observed regardless of the days after FV infection and whether FV stocks used were contaminated with LDV (16) or not (Fig. 1A), indicating that the differences in NK susceptibility were determined mainly by the intrinsic nature of each target cell line, not by the possibly different activation statuses or subsets of the effector cells.

We therefore analyzed the expression of various ligand molecules that are recognized by inhibitory and activating NK receptors: RAE-1 family proteins, the product of the murine ULBP-like transcript-1 (MULT1) gene, and H60 molecules, all of which interact with the major activating NK receptor NKG2D; and MHC class Ib Qa-1 molecules, encoded by the *H2-T23* locus, that are recognized by both inhibitory NKG2A/CD94 and activating NKG2C/CD94 and NKG2E/CD94 receptor complexes (30, 49). As mouse genes encoding RAE-1 molecules (*Raet1*) are polymorphic and B6 mice express the RAE-1 and -1ε isoforms while other strains, such as BALB/c and NOD, express RAE-1 , -1 , and -1 (22, 30), we utilized the anti-Pan–RAE-1 Ab that reacted with all 5 isoforms.

NK-susceptible YAC-1 and FBL-3 cells both expressed RAE-1 molecules on their surfaces at high levels, while NK-resistant Y57-2C and EL-4 cells lacked the expression of RAE-1 (Fig. 2A). In addition, the most highly NK-susceptible YAC-1 cells expressed other NKG2D ligands, MULT1 and H60, while only low-level expression of MULT1, but not H60, was detectable on FBL-3 cells. As YAC-1 cells were established from an A/Sn mouse and FBL-3 from a B6 mouse, the above results are consistent with the fact that B6 mice lack the expression of H60 (22). All three cell lines (FBL-3, Y57-2C, and EL-4) established from an $H2^b$-possessing strain of mice constitutively expressed the product of the $H2\text{-}T23^d$ ($Qa\text{-}1^b$) allele, while YAC-1 cells homozygous for the $H2^a$ haplotype lacked the expression of Qa-1^b.

As the expression of RAE-1 family molecules, as well as Qa-1, is inducible and *Raet1* genes are induced by IFN- (8), which plays a crucial role in immune protection against FV infection (7, 31, 32, 42), we also examined the possible changes in the expression levels of genes encoding these ligands after IFN- stimulation. As predicted, only the F-MuLV-infected leukemia cells, FBL-3 and Y57-2C, expressed transcripts from the viral *env* gene, and their expression levels were markedly enhanced after stimulation with IFN- (Fig. 2B). Stimulation of the two NK-susceptible lines of cells with IFN- resulted in a rapid rise in the levels of the *Raet1* messages; however, no significant expression of the *Raet1* messages was detected in Y57-2C and EL-4 cells even after IFN- stimulation, confirming the lack of expression of RAE-1 in these NK-resistant cell lines. The expression levels of the $Qa\text{-}1^b$ allele in FBL-3 and Y57-2C cells increased after IFN- stimulation, as has been reported previously (14), but YAC-1 cells again lacked the expression of the $Qa\text{-}1^b$ message.

NK killing of FBL-3 target cells was mediated via the NKG2D receptor. To directly assess the above-indicated putative correlation between the expression of NKG2D ligand RAE-1 molecules and susceptibility to killing by NK cells, two monoclonal Abs that block the interaction between NKG2D and its ligands (13, 29) were added separately to the wells of killing assays. The lysis of FBL-3 target cells by NK cells purified from FV-infected $CB6F_1$ mice was abrogated to the levels of that against NK-resistant EL-4 cells by the addition of either of the blocking Abs in repeated experiments (Fig. 2C). The killing of YAC-1 cells was also blocked, at least partially, by the anti-NKG2D Ab, but significant lytic activities were detectable at higher effector-to-target ratios even in the presence of the anti-NKG2D Ab, consistent with the previous finding that YAC-1 cells are killed by NK cells through both NKG2D-dependent and -independent signaling pathways (17). Thus, the results shown in Fig. 1A and 2 collectively indicate that NK cells purified from FV-infected $CB6F_1$ mice recognize F-MuLV-induced FBL-3 target cells mainly through the NKG2D–RAE-1 interactions.

Expansion of NKG2D$^+$ cells and induction of NKG2D ligand expression on infected erythroid progenitor cells in the spleens of FV-inoculated mice. We next examined the possible changes in percentages and absolute numbers of NKG2D cells in the spleens of FV-infected mice. Since NKG2D is known to be expressed by NK as well as a population of CD8 effector cells (17), the percentages of NKG2D cells among CD8 T cells were also analyzed. The percentages of CD3 CD8 T cells in the spleen significantly decreased by 12 days after FV infection (Fig. 1B); however, as total numbers of spleen cells increased following FV infection, absolute numbers of CD3 CD8 T cells did not change significantly during the 12-day period of acute FV infection. On the other hand, absolute numbers of DX5 NKG2D cells started to increase by PID 8 and became significantly higher than those prior to infection at PID 12. Thus, NK cells expanded upon FV infection. Interestingly, significant percentages and numbers of

FIG. 2. Correlation between the expression of different NK receptor ligands and susceptibility to NK killing of 4 different cell lines. (A) Cell surface expression of NK receptor ligands and F-MuLV gp70 on the 4 lines of cells were analyzed by flow cytometry. Shown here are histograms, with each horizontal axis showing fluorescence intensity observed with the indicated Ab. Dotted lines indicate reactivity of isotype control Ab. (B) Real-time PCR quantification of the expression levels of NK receptor ligand genes. Indicated cells were cultured in the presence of 5 U/ml IFN- , and total RNA was extracted at the indicated time points after the stimulation. Specificity of each of the primer sets was confirmed by separate plasmid cloning and sequencing of the amplified DNA fragments. The levels of expression of each tested gene are shown by 2^{-CT} values by using *GAPDH* as a normalizer. Results shown here are mean SEM calculated with data from 2 or 4 reaction wells for each sample dilution. The experiments were repeated 4 times with essentially the same results. (C) Blocking of NK-mediated killing by the anti-NKG2D Ab. Effector NK cells were purified from $CB6F_1$ mice at 8 days after inoculation with FV and confirmed to be 85% positive for both NK-1.1 and DX5. Blocking CX5 (top) or C7 (bottom) Ab (filled symbols) and each corresponding isotype control Ab (open symbols) were added at a final concentration of 30 l/ml according to the previous report (13). The optimality of the above working concentration was confirmed in preliminary experiments. Each data point here represents a mean calculated from quadruplicated wells, with the SEM being 10% of the average throughout the present study. The blocking experiments were repeated 4 times with each Ab and showed essentially the same results.

DX5 NKG2D NK cells were present in the spleens of $CB6F_1$ mice even before FV infection, consistent with the high baseline NK activities detectable in $CB6F_1$ mice (Fig. 1A). The proportion of NKG2D cells among CD8 T cells remained low until PID 8, but the absolute numbers of NKG2D CD8 cells abruptly increased by PID 12.

As to the expression of NKG2D ligands on FV-infected cells *in vivo*, flow cytometric analyses revealed increased expression of RAE-1 and MULT1, but not H60, on the surfaces of gp70 and TER-119 erythroid progenitor cells in the spleens of FV-infected $CB6F_1$ mice (Fig. 3A). As shown in Fig. 3A, gp70 cells were only slightly increased in the spleen until PID 8. Nevertheless, 1/5 of the gp70 cells expressed RAE-1 above the level of the demarcation line, while a large majority of gp70 cells were also negative for RAE-1. By PID 12, gp70 populations increased drastically, and a significant proportion of them expressed RAE-1 above the level of the demarcation line. At the same time point, three distinctive populations of gp70 cells with undetectable levels of TER-119 expression (TER-119 gp70 cells), low levels of TER-119 and high gp70 expression (TER-119^{Lo} $gp70^{Hi}$ cells, purple dots, Fig. 3A), and TER-119^{Hi} gp70 erythroblasts (red dots, Fig. 3A) appeared in the spleen. Based on a previous report (50), these three populations of gp70 cells most likely represent distinctive stages of erythroid cell differentiation from FV-infected progenitor cells, including primitive erythroid progenitor cells and proerythroblasts (TER-119), proerythroblasts and early basophilic erythroblasts (TER-119^{Lo}), and maturing benzidine-positive erythroblasts (TER-119^{Hi}). Importantly, the TER-119^{Lo} population that showed higher levels of gp70 expression than the two other populations also showed higher levels of RAE-1 and MULT1 expression on their surfaces, but their levels of H60 expression were below the detection limit (Fig. 3A).

When mean fluorescence intensities were compared between different populations of spleen cells, the average levels of RAE-1 expression on the surfaces of gp70 cells were significantly higher than those on gp70 cells in $CB6F_1$ mice at all time points tested (Fig. 4). Further, TER-119^{Lo} proerythroblasts and early basophilic erythroblasts expressed significantly higher levels of RAE-1 on their surfaces than TER-119 cells at PID 12, indicating that FV-infected erythroid cells can become susceptible to NK killing due to RAE-1 upregulation.

Decreased MHC class I and class Ib antigen expression on terminally differentiating erythroid cells. The target-killing activities of NK cells are regulated not only by the above positive signals but also by negative signals generated by receptors binding to MHC molecules, and the MHC class Ib Qa-1^b molecule is a strong inhibitor of NK activities in mice (49). Thus, FV-infected erythroid cells might also become susceptible to NK killing due to their possibly reduced expression of class I and/or class Ib molecules. As shown in Fig. 3B, the TER-119 population of spleen cells retained high levels of MHC class I K^b and lower levels of D^b molecules, as well as class Ib Qa-1^b, on their surfaces until PID 12; however, decreased expression of Qa-1^b, as well as K^b and D^b, was discernible in a small population of TER-119 erythroid cells at PID 4 and 8 (data not shown). At PID 12, TER-119^{Hi} terminally differentiating erythroid cells (Fig. 3B, pink dots) showed markedly diminished expression of the class I molecules, and Qa-1^b expression on the majority of TER-119^{Hi} cells became barely detectable. It is notable, however, that the TER-119^{Lo} cells that showed increased expression of RAE-1 (Fig. 3A) retained unchanged levels of class I and Qa-1^b expression, and the lack of Qa-1^b expression was observed only with the TER-119^{Hi} population. As levels of RAE-1 and MULT1 expression, as well as those of viral gp70, on the surfaces of TER-119^{Hi} cells were also reduced in comparison with those on TER-119^{Lo} cells at PID 12 (Fig. 3A), these observations may reflect the global downregulation of gene expression in terminally differentiating erythroid cells (33, 40). Thus, $gp70^{Hi}$ TER-119^{Lo} erythroblasts that are massively increased in the spleen by PID 12 express higher levels of RAE-1 and MULT1 but retain the expression of Qa-1^b.

***In vivo* role of NKG2D–RAE-1 interactions in controlling early expansion of FV-infected cells and the development of virus-induced pathologies.** Although the above experiments have shown significant expansion of NKG2D NK cells and increased expression of RAE-1 proteins on infected erythroid cells upon FV inoculation, the sufficiency of the levels of RAE-1 expression induced in TER-119^{Lo} erythroid cells to evoke NK-mediated killing in the presence of Qa-1^b can be questioned. In this regard, the Ab-mediated depletion of NK cells from mice immunized with a single-epitope peptide vaccine totally abrogated the protective efficacy of Th cell priming, and NK-depleted mice died as rapidly as unimmunized control mice after FV infection in the previous experiments (16). However, the possible physiological role of NK cells in regulating the early proliferation of FV-infected erythroid cells in unimmunized mice of a susceptible strain has not been analyzed. To address this, we administered anti-asialoGM1 Ab to unimmunized $CB6F_1$ mice and reduced the percentages of DX5 NK-1.1 NK cells in the spleen to 1.2 through PID 4 to 12. In the above NK-depleted mice, the number of FV infectious centers in the spleen drastically increased at as early as PID 6 (Fig. 5A), indicating that NK cells are actually restricting early expansion of FV-infected cells in the spleen. The percentages of gp70 cells in the spleen at 6 days after FV infection also increased significantly in the NK-depleted mice and became 3 times higher than those in the control mice infected without NK depletion (Fig. 5B). As $CB6F_1$ mice are highly susceptible to FV-induced disease development, the percentages of gp70 cells in the spleen increased toward PID 12 in both groups; however, the proportions of gp70 cells further increased in the absence of asialoGM1 cells in comparison with those in the control animals given unimmunized sera. Importantly, NK cell depletion also affected the survival of FV-infected mice: when inoculated with a slightly reduced dose of 50 SFFU, highly susceptible $CB6F_1$ mice still developed the fatal disease and most died by 60 days after FV infection, while NK-depleted $CB6F_1$ mice died significantly more rapidly, with an average survival period that was 9 days shorter than that of the control mice (Fig. 5C). These results indicate that NK cells are not only involved in confining the early expansion of FV-infected erythroid cells, but are contributing to natural resistance to FV-induced disease development in unimmunized animals.

Although the administration of anti-asialoGM1 Ab did not affect CD4 and CD8 T-cell numbers and their functionalities in the previous experiments (16), it is possible that FV-reactive T cells, along with NK cells, might have been affected

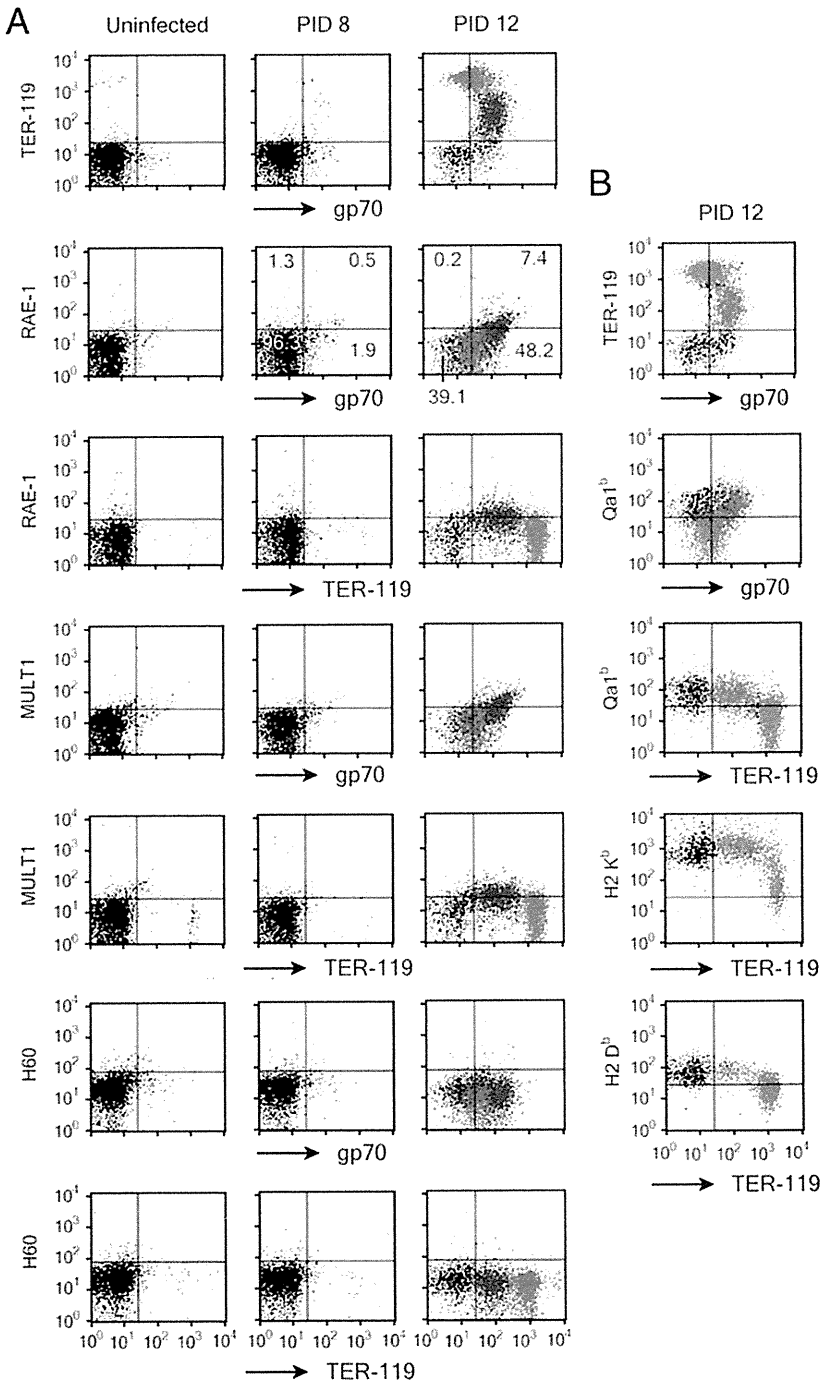

FIG. 3. Representative dot plots showing the expression of NK receptor ligand proteins (A) and MHC class I and class Ib molecules (B) on the surfaces of spleen cells in FV-infected CB6F$_1$ mice. CB6F$_1$ mice were inoculated with 150 SFFU FV, and at least 4 mice were killed at PID 4, 8, and 12 to remove the spleen. Multicolor flow cytometric analyses were performed with each indicated Ab. Uninfected mice were similarly analyzed as controls. Mature erythrocytes and dead cells were excluded by setting a polygonal gate in the dot plots showing intensities of forward scatter and the fluorescence for 7-aminoactinomycin D. Demarcation lines were set based on the fluorescence levels observed by incubating the cells with isotype control Ab. Data on PID 4 are omitted from this figure, as they are essentially similar to those on PID 8, except that gp70 populations are much smaller. In the middle and right panels of the second row of dot plots in panel A, the number in each quadrant represents the percentage of cells that expressed the indicated markers above or below the level of the corresponding demarcation line. Patterns observed with all 4 mice at each time point were consistent with those shown here. In panel A, purple dots, TER-119^{Lo} gp70^{Hi} cells; red dots, TER-119^{Hi} gp70 erythroblasts. In panel B, red dots, TER-119^{Lo} gp70^{Hi} cells; pink dots, TER-119^{Hi} gp70 erythroblasts.

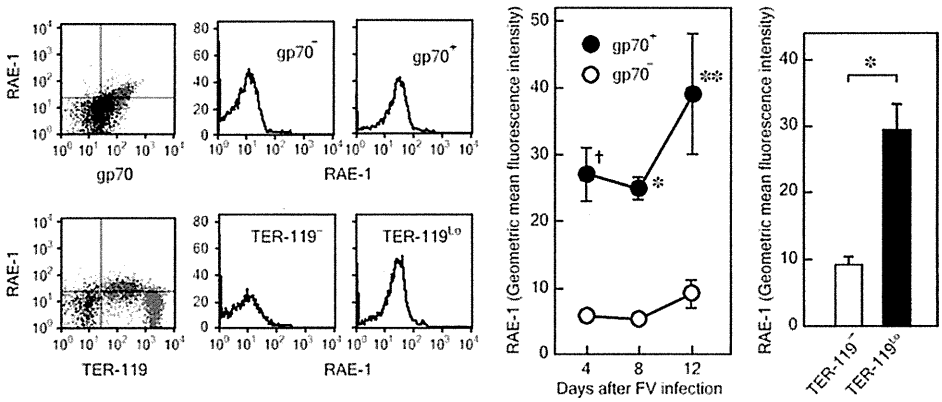

FIG. 4. Different levels of RAE-1 expression between viral gp70-positive and -negative spleen cells in mice infected with FV. $CB6F_1$ mice were inoculated with 150 SFFU of LDV-free FV, and multicolor flow cytometric analyses were performed on nucleated cells as described for Fig. 3. Representative dot plots and histograms on the left show different levels of RAE-1 expression on pairs of gp70 and gp70 or TER-119 and $TER\text{-}119^{Lo}$ populations at PID 12. TER-119 and $TER\text{-}119^{Lo}$ populations are those shown with black and purple dots, respectively, in Fig. 3A. Changes in averages of geometric mean fluorescence intensity (GMFI) for RAE-1 among gp70 and gp70 cells after FV infection are shown in the middle panel. GMFI were calculated by using the region statistics function of the CellQuest software. Each datum shown here is the mean SEM, calculated with GMFI data obtained from 4 mice. Differences between gp70 and gp70 populations were examined by two-way ANOVA with Bonferroni *post hoc* tests: , P 0.05; †, P 0.01; , P 0.001. The right panel shows averages of GMFI for RAE-1 compared between the TER-119 and $TER\text{-}119^{Lo}$ populations at PID 12. Each bar shows mean SEM calculated with GMFI data obtained from 4 or 5 mice. , P 0.02, by paired t test.

by the Ab injections in the above depletion experiments, as activated T cells are known to express asialoGM1 in some viral infections (41). To further demonstrate the direct involvement of the RAE-1 ligand and NKG2D receptor in confining the early expansion of FV-infected cells, blocking Abs were administered to infected $CB6F_1$ mice. The numbers of FV-producing cells in the spleen significantly increased in the animals that were given either NKG2D- or RAE-1-blocking Ab in comparison with those in the control mice (Fig. 5A and D). Further, in the presence of the RAE-1-blocking Ab, FV-infected $CB6F_1$ mice showed significantly larger spleen sizes than control mice (Fig. 5E), confirming that FV-infected erythroid progenitor cells are recognized and their expansion is regulated through NKG2D–RAE-1 interactions *in vivo*. As the effects of the NKG2D or RAE-1 blockade were observed at as early as PID 6, prior to the expansion of NKG2D CD8 T cells (Fig. 1B), it is most likely that mainly NKG2D NK cells were responsible for the above early confinement of FV-induced erythroid cell proliferation.

Increased expression of RAE-1 depends on retroviral replication rather than on erythroid cell proliferation. As the FV complex induces massive proliferation and terminal differentiation of erythroid progenitor cells in mice possessing the *Fv2*^{s} allele, the above-described increase in RAE-1 expression on $TER\text{-}119^{Lo}$ cells may depend on the specific differentiation stage (proerythroblasts and early basophilic erythroblasts) or activated status of red cell precursors, rather than on FV infection. To examine this, we first induced an increased erythropoiesis by administering phenylhydrazine (PHZ) instead of FV infection. After administration of PHZ, both the $TER\text{-}119^{Lo}$ and $TER\text{-}119^{Hi}$ populations became discernible in the spleens of $CB6F_1$ mice; however, neither population in PHZ-treated mice showed increased expression of RAE-1, unlike the gp70 $TER\text{-}119^{Lo}$ population in FV-infected mice (Fig. 6A). Similar results were also obtained for MULT1. Thus, the increase in RAE-1 and MULT1 expression on the $TER\text{-}119^{Lo}$ population was likely caused by FV infection, not by induced erythropoiesis.

To further elucidate putative relationships between FV replication and RAE-1 expression on target cells of FV infection, mice deficient of either of the FV resistance factors APOBEC3 and BAFF-R, which show markedly enhanced FV replication and exaggerated pathology (46, 47), were examined. Mice of the *Fv2*$^{r/r}$ background were utilized so that the effects of FV replication on RAE-1 expression could be further separated from those of SFFV-induced erythroid cell proliferation. Both APOBEC3- and BAFF-R-deficient mice showed markedly increased numbers of gp70-expressing cells in the spleen in comparison with those in the wild-type (WT) animals (Fig. 6B). Importantly, RAE-1-positive cells increased in association with the increased numbers of gp70 cells in APOBEC3- and BAFF-R-deficient animals. In APOBEC3-deficient mice, most of the gp70 cells were TER-119 and B220 , and these cells showed increased expression of RAE-1 proteins on their surfaces (Fig. 6B, arrows). In mice deficient of BAFF-R, even larger numbers of both TER-119 (Fig. 6B, orange dots) and TER-119 cells (Fig. 6B, red dots) were infected with FV, and these gp70 cells expressed higher levels of RAE-1 than gp70 cells. Interestingly, in FV-infected *BAFF-R*$^{-/-}$ mice a significant proportion of B220 B lymphocytes were also infected with FV, and they expressed higher levels of RAE-1 than uninfected B cells (Fig. 6B, blue dots).

As SFFV-induced growth potentiation of erythroid cells is limited in the above-described *Fv2*^{r} B6-background mice and as gp70 B cells, as well as erythroid cells, expressed higher levels of RAE-1 proteins than gp70 cells, the above results suggested that the replication of F-MuLV alone in the absence of SFFV might induce increased RAE-1 expression on target cells. Thus, we next infected the same gene-targeted animals with an infectious molecular clone of F-MuLV. In APOBEC3-

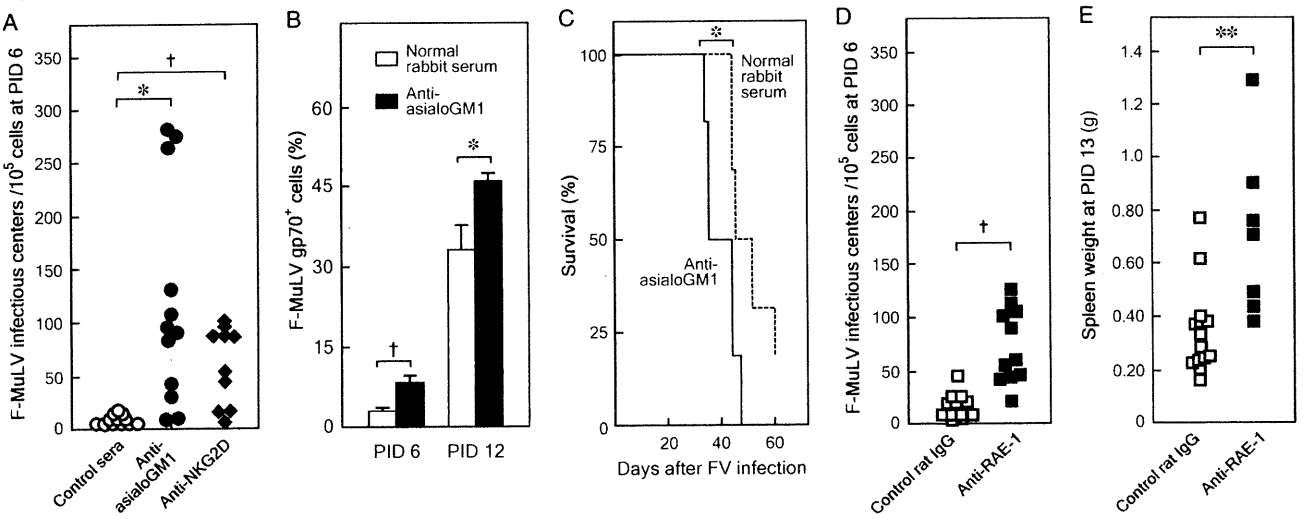

FIG. 5. Effects of the administration of anti-asialoGM1, anti-NKG2D, or anti-RAE-1 Ab on the expansion of virus-producing cells in the spleen and the development of FV-induced pathologies. (A) $CB6F_1$ mice were injected with either the anti-asialoGM1 or the blocking anti-NKG2D Ab and inoculated with 150 SFFU of FV. Control mice were injected with a mixture of normal rabbit and normal rat sera (control sera), and similarly infected. F-MuLV infectious centers in the spleen were enumerated by fluorescent focus assays as described previously (19, 44–47). Each symbol represents a datum from an individual mouse. As the anti-asialoGM1 and anti-NKG2D Ab-injected groups were compared with the common control group given the mixture of unimmunized sera, Bonferroni's correction was performed for multiple comparisons: , P 0.0028 (0.05) 0.0253; †, P 0.0005 (0.05) 0.0253 by Welch's t test. (B) $CB6F_1$ mice were injected with the anti-asialoGM1 Ab as described previously (16) and inoculated with 150 SFFU of FV. Percentages of NK cells expressing both DX5 and NK-1.1 markers among spleen cells were monitored by multicolor flow cytometry as shown in Fig. 1, inset, and percentages of gp70 cells were determined by the specific binding of Ab 720 at the indicated time points. Data shown here are mean SEM calculated with values obtained from 5 to 12 animals per group at each time point. Comparisons were made between the anti-asialoGM1-treated and control groups: , P 0.03; †, P 0.005 by Welch's t test. (C) Survival of anti-asialoGM1-treated animals (n 6) after FV infection compared with that of control mice given normal rabbit serum (n 6). As $CB6F_1$ mice are highly susceptible to FV and most died within 60 days after inoculation with as low as 15 SFFU in a previous experiment (16), a slightly lower dose of 50 SFFU was selected here in an attempt to detect the possibly increased susceptibility in NK-depleted mice. Two survival curves were compared by Mantel-Cox log-rank test: , P 0.026. (D and E) Groups of $CB6F_1$ mice were injected with either the RAE-1-bloking Ab (49) or control rat IgG and inoculated with 150 (D) or 50 SFFU (E) of FV. Spleen infectious centers were enumerated at PID 6 as described previously (19, 44–47), separate groups were killed at PID 13, and their spleen weights measured. The slightly reduced dose was utilized for the experiment shown in panel E, for the sake of consistency with the survival experiment described in the legend to panel C. Each symbol represents a datum from an individual mouse. †, P 0.0005 by Welch's t test; , P 0.0028 by Student's t test.

deficient mice, a large proportion of TER-119 cells were infected and expressed gp70; however, unlike the TER-119 gp70 cells in the same gene-targeted mice infected with FV complex, these cells showed only a slight increase in RAE-1 expression (Fig. 7A, arrows). Similar effects of the absence of the SFFV component on the expression of RAE-1 in erythroid cells were more evidently observed with BAFF-R-deficient mice: TER-119 cells were infected with F-MuLV and expressed gp70, but unlike the same population of erythroid cells in FV-infected mice, these cells did not show a marked increase in the expression of RAE-1 proteins on their surfaces (Fig. 7A, orange dots). On the other hand, B220 B cells in F-MuLV-infected *BAFF-R* ′ mice (Fig. 7A, blue dots) showed increased expression of RAE-1 as observed upon FV infection.

To further confirm the above differences in RAE-1 expression levels between erythroid cells and B lymphocytes upon FV and F-MuLV infections, TER-119 and B220 cells were gated and their expression levels of RAE-1 proteins were compared between gp70 and gp70 populations. When infected with the FV complex, the gp70 populations of both TER-119 and B220 cells expressed significantly higher levels of RAE-1 than the corresponding gp70 cells in both APOBEC3- and BAFF-R-deficient animals (Fig. 7B). The average levels of RAE-1 expression on gp70 cells were 2.69 0.12 and 3.28 0.26 times higher than those on gp70 cells among TER-119 and B220 cell populations, respectively, in FV-infected BAFF-R-deficient mice. On the other hand, although levels of RAE-1 expression between gp70 and gp70 populations were significantly different, gp70 cells among TER-119 erythroid cells in F-MuLV-infected BAFF-R-deficient mice expressed on their surfaces a level of RAE-1 proteins only 1.47 0.06 times higher than that of gp70 cells, while RAE-1 expression in the gp70 population of B220 B lymphocytes became even higher than that observed with FV-infected mice. In fact, the average level of RAE-1 expression on gp70 cells among B220 cells was 4.54 0.13 times higher than that on gp70 cells. Thus, these results indicate that SFFV is required for highly increased expression of RAE-1 on TER-119 erythroid cells, while replication of F-MuLV alone induces increased RAE-1 expression in B220 B cells.

DISCUSSION

As we have shown here, NKG2D NK cells expanded in the spleen and the levels of RAE-1 expression became preferentially higher on the surfaces of viral gp70-expressing cells in FV-infected mice. Although we have not tested all known

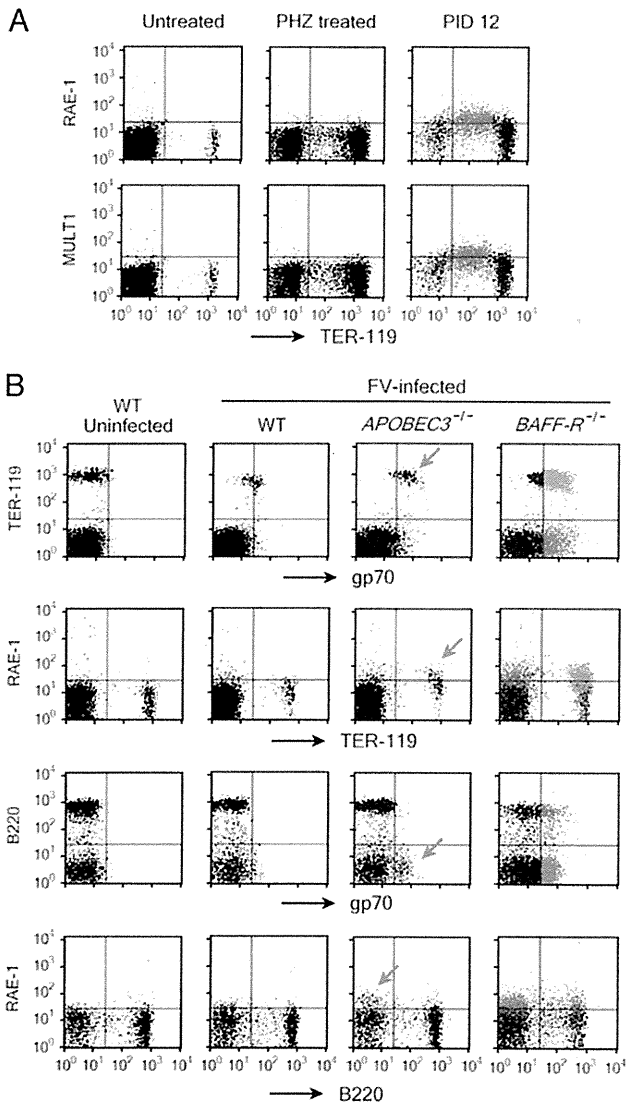

FIG. 6. RAE-1 expression on erythroid progenitor cells is induced by FV infection, not by erythropoiesis. (A) Representative dot plots showing the expression of NK receptor ligand proteins on the surfaces of nucleated spleen cells in phenylhydrazine-treated $CB6F_1$ mice. $CB6F_1$ mice were either injected with 1.2 mg/mouse PHZ on days 0 and 1 or inoculated with 150 SFFU FV on day 0, and at least 4 mice were killed on day 5 or day 12, respectively, to remove the spleen. Multicolor flow cytometric analyses were performed on nucleated cells with each indicated Ab. Demarcation lines were set based on the fluorescence levels observed by incubating the cells with isotype control Ab. Patterns observed with all 4 mice for each experimental group were consistent with those shown here. (B) Representative dot plots showing the expression of viral gp70, RAE-1, erythroid marker TER-119, and B-cell marker B220 on the surfaces of nucleated spleen cells in FV-infected B6 mice lacking an FV-resistance factor. As *Fv2*$^{r/r}$ mice were utilized, they were infected with 5 10^4 SFFU of FV complex, and 4 to 5 mice for each group were killed to remove the spleen. Flow cytometric analyses were performed as described in the legend to Fig. 3. Representative data obtained at PID 10 are shown here. In panel A, red dots, TER-119^{Lo} $gp70^{Hi}$ cells. In panel B, red dots, TER-119 gp70 cells; orange dots, TER-119 gp70 cells; purple dots, B220 gp70 cells; blue dots, B220 gp70 cells in FV-infected *BAFF-R*$^{-/-}$ mice.

ligands for NK cell receptors, the nearly complete abrogation of the killing activities against F-MuLV-induced FBL-3 target cells exerted by DX5 cells purified from FV-infected $CB6F_1$ mice *in vitro* and the significant increase in the number of FV infectious centers *in vivo* in the presence of the NKG2D-blocking Ab clearly indicate that the NKG2D receptor is involved primarily in the recognition and elimination of infected erythroid cells in FV-inoculated animals. Further, although the levels of induction of RAE-1 proteins on the surfaces of gp70 erythroid cells were relatively low, as detectable by flow cytometry with the currently utilized Ab, and the same gp70 TER-119^{Lo} cells retained Qa-1^b molecules on their surfaces, the induced RAE-1 proteins are apparently sufficient to induce the elimination of FV-infected erythroid cells *in vivo*, as the administration of the RAE-1-blocking Ab resulted in significantly increased numbers of infectious centers and more pronounced splenomegaly after FV inoculation. In this regard, FBL-3 cells were killed efficiently by purified NK cells despite their expression of Qa-1^b on the surfaces. Thus, NKG2D–RAE-1 interactions are involved in the elimination of virus-infected cells in the early stages of FV infection *in vivo*. These results are consistent with the previous finding that overexpression of VEGF-A paradoxically resulted in delayed development of FV-induced leukemia, probably due partly to enhanced NK cell activities in the transgenic mice (4).

The mechanisms by which FV infection upregulates the expression of RAE-1 molecules in erythroid progenitor cells and B lymphocytes are currently unknown. Several cytokines, including IFN- , have been shown to upregulate the expression of these retinoid-inducible genes (8, 49), and we have demonstrated in the present study that IFN- augments the expression of *Raet1* genes in F-MuLV-induced leukemia cells. As the production of IFN- in the spleens of FV-infected mice has been detected at as early as 5 days after virus inoculation (31), the induction of *Raet1* gene expression in FV-infected cells might be mediated by IFN- . However, as higher levels of RAE-1 proteins were expressed preferentially on gp70 cells, it is unlikely that cytokine-mediated induction, which should work on both FV-infected and uninfected cells in the spleen, is responsible mainly for the increased levels of RAE-1 protein expression on FV-infected cells. The lack of increased RAE-1 expression on TER-119^{Lo} cells in PHZ-injected mice also indicates the presence of a virus-specific, rather than a differentiation- or growth-associated, mechanism of RAE-1 induction. In this regard, infection of mouse primary B lymphocytes with highly leukemogenic Abelson MuLV induces the expression of activation-induced cytidine deaminase (AID), and the genotoxic action of AID leads to upregulation of NKG2D ligands on infected cell surfaces (11). HIV-1 Vpr is also known to upregulate the expression of NKG2D ligands on cell surfaces (35), and the above Vpr-induced upregulation of NKG2D ligand expression has been shown to be mediated through the DNA damage response (48). Thus, it is tempting to speculate that repeated proviral integrations into the erythroid progenitor cells that are facilitated in the presence of SFFV-induced growth potentiation may cause DNA damage and the resultant upregulation of RAE-1 expression in FV-infected erythroid cells.

Taking advantage of known FV-resistant host factors (5, 12, 25, 27, 46, 47), we successfully dissected here the effect of

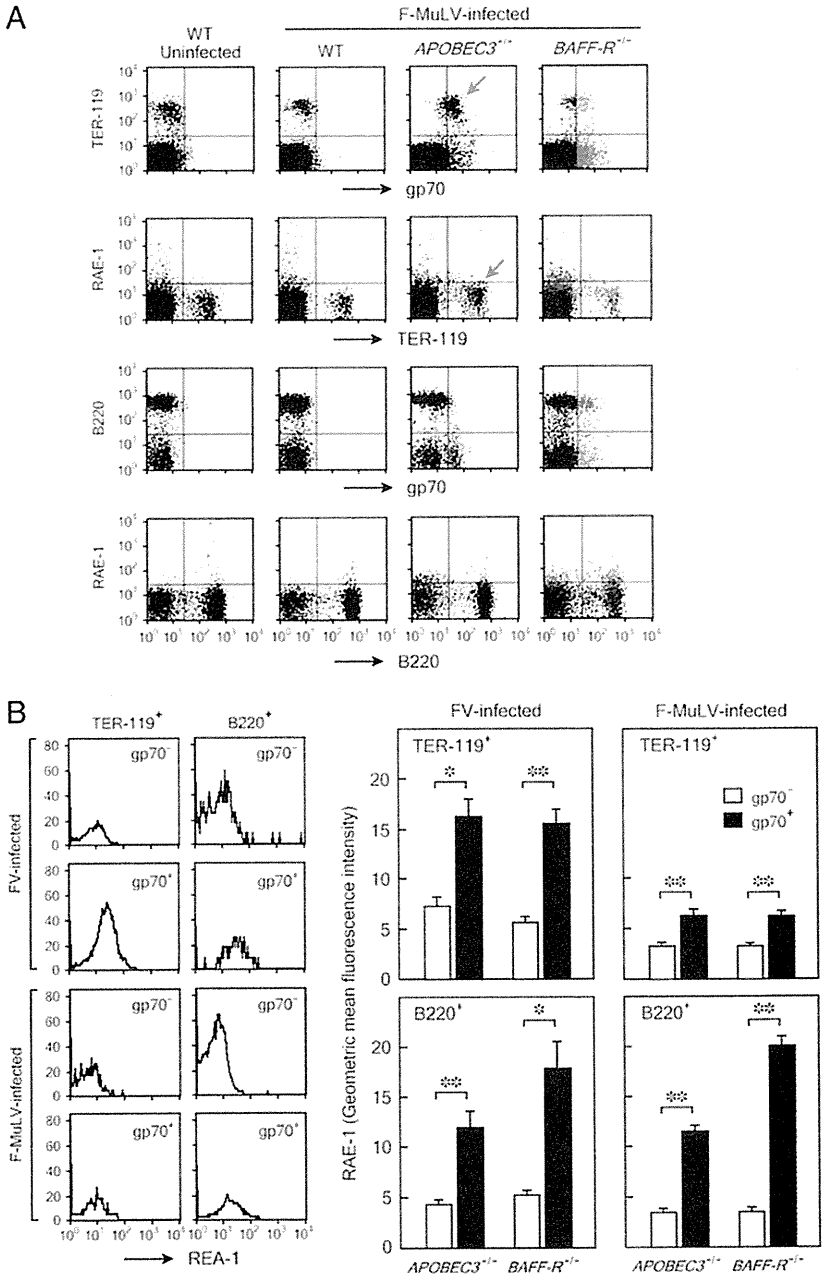

FIG. 7. RAE-1 expression on spleen cells upon infection with F-MuLV alone. (A) Representative dot plots showing the expression of viral gp70, RAE-1 proteins, TER-119, and B220 on the surfaces of nucleated spleen cells in F-MuLV-infected B6 mice lacking an FV resistance factor. Mice were infected with 5 10^4 fluorescent focus units of F-MuLV (FB-29), and 4 or 5 mice for each group were killed to remove the spleen. Flow cytometric analyses were performed as described for Fig. 3. Representative data obtained at PID 10 are shown here. Arrows, slight increase in RAE-1 expression on the surfaces of TER-119 gp70 cells in F-MuLV-infected *APOBEC3* mice. Red dots, TER-119 gp70 cells; orange dots, TER-119 gp70 cells; purple dots, B220 gp70 cells; blue dots, B220 gp70 cells in F-MuLV-infected *BAFF-R* mice. (B) Representative histograms on the left show different levels of RAE-1 expression on gp70 and gp70 populations of TER-119 erythroid and B220 B cells. Averages of GMFI for RAE-1 compared between the gp70 and gp70 populations of TER-119 erythroid cells and B220 B lymphocytes are shown on the right. Each bar shows mean SEM calculated with GMFI data obtained from 4 or 5 mice. , P 0.02; , P 0.004 by paired t test.

SFFV-induced erythroid cell growth potentiation from that of FV replication on RAE-1 induction in target cells. In fact, FV infection in the absence of massive erythroid cell proliferation still resulted in highly increased RAE-1 expression on TER-119 erythroid cells in *Fv2* B6 mice lacking either APOBEC3 or BAFF-R. Highly increased expression of RAE-1 on infected erythroid as well as B cells in the gene-targeted B6 mice indicates a close correlation between high levels of retroviral rep-

lication and induction of RAE-1 expression on target cells. It should be noted, however, that although B cells expressed similarly increased levels of RAE-1 proteins upon infection with FV complex or with F-MuLV alone, levels of RAE-1 induction on erythroid cells became much higher in the presence of the SFFV component. Thus, in the above conditions of nonrestricted retroviral replication, F-MuLV alone can induce RAE-1 expression in B cells, while SFFV is also required for the induction of high levels of RAE-1 in erythroid cells. In fact, SFFV-induced growth potentiation of infected erythroid cells in the *Fv2*^{s}-possessing CB6F$_1$ mice further enhanced RAE-1 expression on gp70 erythroblasts, as RAE-1 levels on gp70 cells in CB6F$_1$ mice were apparently higher than those in the gene-targeted B6 mice (compare fluorescence intensities between Fig. 4 and 7). Nevertheless, the above cell type-associated differences in RAE-1 expression in F-MuLV-infected B6 mice may facilitate further dissection of viral and cellular factors that are involved in retrovirus-induced RAE-1 upregulation.

In the present study, we observed a lag in the increase of TER-119 erythroblasts until PID 8, followed by an abrupt and massive increase of gp70 cells in the spleen by PID 12. An abrupt increase in the number of TER-119 cells in the spleen starting around PID 8 has repeatedly been observed with *Fv2*^{s}-possessing mice (16, 19, 26), which is consistent with a recent finding of two distinctive populations of target cells for FV infection (43). Thus, one population expresses the short-form STK and generates erythropoietin-independent erythroid burst-forming units (BFU-E) in the bone marrow soon after FV infection, while cells of the other population migrate into the spleen as infectious centers, interact with the stromal cells to express bone morphogenic protein 4, and cause the expansion of stress BFU-E. It is tempting to speculate that the cells expressing increased levels of RAE-1 and MULT1 are FV-infected stress BFU-E and that they are susceptible to NK killing. As the depletion of NK cells or the blockade of either NKG2D or RAE-1 resulted in significantly increased FV infectious centers in the spleen at as early as PID 6, followed by significantly more pronounced splenomegaly and earlier death, it is also possible that NK cells are restricting the migration of CD31 Kit CD41 Sca1 Lin infectious center cells into the spleen. In fact, immunization of mice with the gp70-derived Th-cell epitope suppressed the above abrupt expansion of TER-119 cells in the spleen that otherwise started from PID 8 (16, 19, and 26), and this vaccine effect was abrogated by depletion of NK cells (16), indicating that Th cell-mediated activation of NK cells may have suppressed the migration of FV infectious centers from bone marrow. Thus, this model may also shed light on basic mechanisms through which the migration of committed erythroid progenitor cells from bone marrow to the spleen might be regulated by NK cell functions.

ACKNOWLEDGMENTS

This work was supported in part by grants-in-aid from the Ministry of Education, Culture, Sports, Science, and Technology of Japan, including the High-Tech Research Center, Medico-Technical Cooperation, and Anti-Aging Center grants, those from the Ministry of Health, Labor, and Welfare of Japan for Research on HIV/AIDS, and those from the Japan Health Sciences Foundation. The use of radioisotopes, animal experiments, and flow cytometric analyses were supported by members of the Central Research Facilities, Kinki University School of Medicine.

We are grateful to J. Brian Dowell for critically reading and correcting the manuscript and to Yoshiko Ito, Department of Respiratory Medicine and Allergology, Kinki University School of Medicine, for her help in operating the AutoMACS.

REFERENCES

1. Alter, G., et al. 2007. Evolution of innate and adaptive effector cell functions during acute HIV-1 infection. J. Infect. Dis. 195:1452–1460.
2. Arase, H., T. Saito, J. H. Phillips, and L. L. Lanier. 2001. Cutting edge: the mouse NK cell-associated antigen recognized by DX5 monoclonal antibody is CD49b ($_2$ integrin, very late antigen-2). J. Immunol. 167:1141–1144.
3. Azakami, K., et al. 2009. Severe loss of invariant NKT cells exhibiting anti-HTLV-1 activity in patients with HTLV-1-associated disorders. Blood 114:3208–3215.
4. Cervi, D., et al. 2007. Enhanced natural-killer cell and erythropoietic activities in VEGF-A-overexpressing mice delay F-MuLV-induced erythroleukemia. Blood 109:2139–2146.
5. Chesebro, B., M. Miyazawa, and W. J. Britt. 1990. Host genetic control of spontaneous and induced immunity to Friend murine retrovirus infection. Annu. Rev. Immunol. 8:477–499.
6. Costello, R. T., C. Fauriat, S. Sinori, E. Marcenaro, and D. Olive. 2004. NK cells: innate immunity against hematopoietic malignancies? Trends Immunol. 26:328–333.
7. Dittmer, U., et al. 2001. Role of interleukin-4 (IL-4), IL-12, and gamma interferon in primary and vaccine-primed immune responses to Friend retroviral infection. J. Virol. 75:654–660.
8. Faria, P. A., et al. 2005. VSV disrupts the Rae1/mrnp41 mRNA nuclear export pathway. Mol. Cell 17:93–102.
9. Gaudieri, S., et al. 2005. Killer immunoglobulin-like receptors and HLA act both independently and synergistically to modify HIV disease progression. Genes Immun. 6:683–690.
10. Giavedoni, L. D., M. C. Velasquillo, L. M. Parodi, G. B. Hubbard, and V. L. Hodora. 2000. Cytokine expression, natural killer cell activation, and phenotypic changes in lymphoid cells from rhesus macaques during acute infection with pathogenic simian immunodeficiency virus. J. Virol. 74:1648–1657.
11. Gourzi, P., T. Leonova, and F. N. Papavasiliou. 2006. A role for activation-induced cytidine deaminase in the host response against a transforming retrovirus. Immunity 24:779–786.
12. Hasenkrug, K. J., and B. Chesebro. 1997. Immunity to retroviral infection: the Friend virus model. Proc. Natl. Acad. Sci. U. S. A. 94:7811–7816.
13. Ho, E. L., et al. 2002. Costimulation of multiple NK cell activation receptors by NKG2D. J. Immunol. 169:3667–3675.
14. Howcroft, T. K., and D. S. Singer. 2003. Expression of nonclassical MHC class Ib genes: comparison of regulatory elements. Immunol. Res. 27:1–30.
15. Iannello, A., O. Debbeche, S. Samarani, and A. Ahmad. 2008. Antiviral NK cell responses in HIV infection. I. NK cell receptor genes as determinants of HIV resistance and progression to AIDS. J. Leuko. Biol. 84:1–26.
16. Iwanami, N., A. Niwa, Y. Yasutomi, N. Tabata, and M. Miyazawa. 2001. Role of natural killer cells in resistance against Friend retrovirus-induced leukemia. J. Virol. 75:3152–3163.
17. Jamieson, A. M., et al. 2002. The role of the NKG2D immunoreceptor in immune cell activation and natural killing. Immunity 17:19–29.
18. Kabat, D. 1989. Molecular biology of Friend viral erythroleukemia. Curr. Top. Microbiol. Immunol. 148:1–42.
19. Kawabata, H., et al. 2006. Peptide-induced immune protection of CD8 T cell-deficient mice against Friend retrovirus-induced disease. Int. Immunol. 18:183–198.
20. Kina, T., et al. 2000. The monoclonal antibody TER-119 recognizes a molecule associated with glycophorin A and specifically marks the late stages of murine erythroid lineage. Br. J. Haematol. 109:280–287.
21. Kottilil, S., et al. 2003. Innate immunity in human immunodeficiency virus infection: effect of viremia on natural killer cell function. J. Infect. Dis. 187:1038–1045.
22. Maier, L. M., et al. 2008. NKG2D–RAE-1 receptor-ligand variation does not account for the NK cell defect in Nonobese diabetic mice. J. Immunol. 181:7073–7080.
23. Martin, M. P., et al. 2002. Epistatic interaction between KIR3DS1 and HLA-B delays the progression to AIDS. Nat. Genet. 31:429–434.
24. Martin, M. P., et al. 2007. Innate partnership of HLA-B and KIR3DL1 subtypes against HIV-1. Nat. Genet. 39:733–740.
25. Miyazawa, M. 2004. Host genes that influence immune and non-immune resistance mechanisms against retroviral infections. Rec. Res. Dev. Virol. 6:105–118.
26. Miyazawa, M., et al. 1995. Immunization with a single T helper cell epitope abrogates Friend virus-induced early erythroid proliferation and prevents late leukemia development. J. Immunol. 155:748–758.
27. Miyazawa, M., S. Tsuji-Kawahara, and Y. Kanari. 2008. Host genetic factors that control immune responses to retrovirus infections. Vaccine 26:2981–2996.

28. Ney, P. A., and A. D. D'Andrea. 2000. Friend erythroleukemia revisited. Blood 96:3675–3680.
29. Ogasawara, K., et al. 2004. NKG2D blockade prevents autoimmune diabetes in NOD mice. Immunity 20:757–767.
30. Ogasawara, K., and L. L. Lanier. 2005. NKG2D in NK and T cell-mediated immunity. J. Clin. Immunol. 25:534–540.
31. Peterson, K. E., M. Iwashiro, K. J. Hasenkrug, and B. Chesebro. 2000. Major histocompatibility complex class I gene controls the generation of gamma interferon-producing CD4 and CD8 T cells important for recovery from Friend retrovirus-induced leukemia. J. Virol. 74:5363–5367.
32. Peterson, K. E., I. Stromnes, R. Messer, K. Hasenkrug, and B. Chesebro. 2002. Novel role of CD8 T cells and major histocompatibility complex class I genes in the generation of protective CD4 Th1 responses during retrovirus infection in mice. J. Virol. 76:7942–7948.
33. Pradet-Balade, B., C. Leberbauer, N. Schweifer, and F. Boulmé. 2010. Massive translational repression of gene expression during mouse erythroid differentiation. Biochim. Biophys. Acta 1799:630–641.
34. Ravet, S., et al. 2007. Distinctive NK-cell receptor repertoires sustain high-level constitutive NK-cell activation in HIV-exposed uninfected individuals. Blood 109:4296–4305.
35. Richard, J., S. Sindhu, T. N. Pham, J. P. Belzile, and E. A. Cohen. 2010. HIV-1 Vpr up-regulates expression of ligands for the activating NKG2D receptor and promotes NK cell-mediated killing. Blood 115:1354–1363.
36. Robertson, M. N., et al. 1991. Production of monoclonal antibodies reactive with a denatured form of the Friend murine leukemia virus gp70 envelope protein: use in a focal infectivity assay, immunohistochemical studies, electron microscopy and Western blotting. J. Virol. Methods 34:255–271.
37. Sasaki, Y., S. Casola, J. L. Kutok, K. Rajewsky, and M. Schmidt-Supprian. 2004. TNF family member B cell-activating factor (BAFF) receptor-dependent and -independent roles for BAFF in B cell physiology. J. Immunol. 173:2245–2252.
38. Scott-Algara, D., et al. 2003. Increased NK cell activity in HIV-1-exposed but uninfected Vietnamese intravenous drug users. J. Immunol. 171:5663–5667.
39. Seaman, W. E. 2000. Natural killer cells and natural killer T cells. Arthritis Rheum. 43:1204–1217.
40. Sieff, C., et al. 1982. Changes in cell surface antigen expression during hemopoietic differentiation. Blood 60:703–713.
41. Slifka, M. K., R. R. Pagarigan, and J. L. Whitton. 2000. NK markers are expressed on a high percentage of virus-specific CD8 and CD4 T cells. J. Immunol. 164:2009–2015.
42. Stromnes, I. M., et al. 2002. Temporal effects of gamma interferon deficiency on the course of Friend retrovirus infection in mice. J. Virol. 76:2225–2232.
43. Subramanian, A., et al. 2008. Friend virus utilizes the BMP4-dependent stress erythropoiesis pathway to induce erythroleukemia. J. Virol. 82:382–393.
44. Sugahara, D., S. Tsuji-Kawahara, and M. Miyazawa. 2004. Identification of a protective CD4 T-cell epitope in $p15^{gag}$ of Friend murine leukemia virus and role of the MA protein targeting the plasma membrane in immunogenicity. J. Virol. 78:6322–6334.
45. Takamura, S., et al. 2010. Premature terminal exhaustion of Friend virus-specific effector CD8 T cells by rapid induction of multiple inhibitory receptors. J. Immunol. 184:4696–4707.
46. Takeda, E., et al. 2008. Mouse APOBEC3 restricts Friend leukemia virus infection and pathogenesis in vivo. J. Virol. 82:10998–11008.
47. Tsuji-Kawahara, S., et al. 2010. Persistence of viremia and production of neutralizing antibodies differentially regulated by polymorphic *APOBEC3* and *BAFF-R* loci in Friend virus-infected mice. J. Virol. 84:6082–6095.
48. Ward, J., et al. 2009. HIV-1 Vpr triggers natural killer cell-mediated lysis of infected cells through activation of the ATR-mediated DNA damage response. PLoS Pathog. 5:e1000613.
49. Yokoyama, W. M., and B. F. M. Plougastel. 2003. Immune functions encoded by the natural killer gene complex. Nat. Rev. Immunol. 3:304–316.
50. Zhang, J., M. Socolovsky, A. W. Gross, and H. F. Lodish. 2003. Role of Ras signaling in erythroid differentiation of mouse fetal liver cells: functional analysis by a flow cytometry-based novel culture system. Blood 102:3938–3946.
51. Zhou, R., H. Wei, R. Sun, J. Zhang, and Z. Tian. 2007. NKG2D recognition mediates Toll-like receptor 3 signaling-induced breakdown of epithelial homeostasis in the small intestines of mice. Proc. Natl. Acad. Sci. U. S. A. 104:7512–7515.

OPEN ACCESS Freely available online

PLoS one

TLR2-Dependent Induction of IL-10 and Foxp3$^+$CD25$^+$CD4$^+$ Regulatory T Cells Prevents Effective Anti-Tumor Immunity Induced by Pam2 Lipopeptides *In Vivo*

Sayuri Yamazaki[1*·], Kohei Okada[1·], Akira Maruyama[1], Misako Matsumoto[1], Hideo Yagita[2], Tsukasa Seya[1*]

1 Department of Microbiology and Immunology, Graduate School of Medicine, Hokkaido University, Sapporo, Japan, 2 Department of Immunology, Juntendo University School of Medicine, Tokyo, Japan

Abstract

16 S-[2,3-bis(palmitoyl)propyl]cysteine (Pam2) lipopeptides act as toll-like receptor (TLR)2/6 ligands and activate natural killer (NK) cells and dendritic cells (DCs) to produce inflammatory cytokines and cytotoxic NK activity *in vitro*. However, in this study, we found that systemic injection of Pam2 lipopeptides was not effective for the suppression of NK-sensitive B16 melanomas *in vivo*. When we investigated the immune suppressive mechanisms, systemic injection of Pam2 lipopeptides induced IL-10 in a TLR2-dependent manner. The Pam2 lipopeptides increased the frequencies of Foxp3$^+$CD4$^+$ regulatory T (T reg) cells in a TLR2- and IL-10- dependent manner. The T reg cells from Pam2-lipopeptide injected mice maintained suppressor activity. Pam2 lipopeptides, plus the depletion of T reg with an anti-CD25 monoclonal antibody, improved tumor growth compared with Pam2 lipopeptides alone. In conclusion, our data suggested that systemic treatment of Pam2 lipopeptides promoted IL-10 production and T reg function, which suppressed the effective induction of anti-tumor immunity *in vivo*. It is necessary to develop an adjuvant that does not promote IL-10 and T reg function in vivo for the future establishment of an anti-cancer vaccine.

Citation: Yamazaki S, Okada K, Maruyama A, Matsumoto M, Yagita H, et al. (2011) TLR2-Dependent Induction of IL-10 and Foxp3$^+$CD25$^+$CD4$^+$ Regulatory T Cells Prevents Effective Anti-Tumor Immunity Induced by Pam2 Lipopeptides *In Vivo*. PLoS ONE 6(4): e18833. doi:10.1371/journal.pone.0018833

Editor: Jacques Zimmer, Centre de Recherche Public de la Santé (CRP-Santé), Luxembourg

Received January 28, 2011; Accepted March 10, 2011; Published April 20, 2011

Funding: This work was funded by Grant for challenging exploratory research, Japan Society for The Promotion of Science Challenging Grand (SY), Grants-in-Aid from the Ministry of Education, Science, and Culture (Specified Project for Advanced Research) and the Ministry of Health, Labor, and Welfare of Japan, the Mochida Memorial Foundation for Medical and Pharmaceutical Research (SY), the Yakult Foundation, and the Waxman Foundation. The funders had no role in study design, data collection and analysis, decision to publish, or preparation of the manuscript.

Competing Interests: The authors have declared that no competing interests exist.

* E-mail: seya-tu@pop.med.hokudai.ac.jp (TS); yamazas@med.hokudai.ac.jp (SY)

. These authors contributed equally to this work.

Introduction

Foxp3$^+$CD25$^+$CD4$^+$regulatory T (T reg) cells constitute about 5–10% of peripheral CD4$^+$T cells and control immunological self-tolerance and tumor immunity [1,2]. T reg cells directly infiltrate the tumor and suppress effector cells [3–5]. T reg cells are also induced from non-T reg cells in the draining lymph nodes of tumor-bearing mice by transforming growth factor (TGF)-b producing dendritic cells (DCs) [6]. Effective anti-tumor immunity is induced by depletion of T reg cells with anti-CD25 monoclonal antibody (mAb) [7–9], or blockade of T reg function with anti-CTLA-4 mAb [10–12] or anti-GITR mAb [3]. Specific depletion of T reg cells using mice that express diphtheria toxin receptor under the control of the Foxp3 locus induced tumor regression [4,13]. Therefore, strategies are required to abolish the T reg-induced tolerance that suppresses tumor immunity, thereby establishing an effective anti-tumor immune response.

To overcome the immune suppression mediated by T reg cells in cancer, activation of DCs with adjuvants is required [14,15]. Adjuvants are mainly targeted to pattern recognition receptors, such as Toll like receptor (TLR) ligands on DCs. To date, cancer vaccine adjuvants have included various TLR agonists such as TLR3, TLR4, TLR5, TLR7 and TLR9 [16,17]. DCs stimulated by lipopolysaccharide (LPS), a TLR4 agonist, were found to expand functional T reg cells [18,19]. Hence, it is critical to identify the optimal adjuvants that mature DCs but have less potential to expand T reg cells. However, it is unclear how adjuvants differently affect T reg cell survival and function.

The Bacillus Calmette-Guerin-cell wall skeleton (BCG-CWS) is a TLR2 agonist [20] and has been used as an effective adjuvant for cancer for almost 40 years [16,21]. However, its clinical usage is limited since BCG-CWS is a large molecular complex unable to be chemically synthesized with full activity. The anti-cancer activity of BCG-CWS operates partly through TLR2 signal [22–24], hence, we investigated the adjuvant activity of synthetic TLR2/TLR6 ligands derived from *Staphylococcus aureus*, 16 S-[2,3-bis(palmitoyl)propyl]cysteine (Pam2) lipopeptides. We have previously reported that Pam2 lipopeptides activate DCs and natural killer (NK) cells to produce interferon (IFN)- c and killer activity *in vitro* [25] and that local injection of Pam2 lipopetides with

RGDS peptides, plus tumor extract, could inhibit tumor growth [26].

Here, we tested if systemic injection of Pam2 lipopeptides in mice could induce an effective anti-tumor immune response. The Pam2 lipopeptides have two palmitoyl-bases attached to different peptide sequences (Fig. 1A) and the peptide portion determines the activity of the TLR2 agonist [25]. We selected the most effective TLR2 activators among the 20 Pam2 lipopeptides [25] and investigated the corresponding anti-tumor response *in vivo*. In contrast with the *in vitro* results, systemic injection of Pam2 lipopeptides did not induce regression of NK-sensitive melanomas. Pam2 lipopeptides induced IL-10 and the expansion of T reg cells *in vivo* in a TLR2-dependent manner. We also found that the depletion of T reg cells by treatment with an anti-CD25 mAb before Pam2 lipopeptide injection, suppressed the tumor growth compared with Pam2-lipopeptide injection alone. These data suggested that systemic injection of Pam2 lipopeptides induced IL-10 and T reg cells, preventing effective tumor immunity *in vivo*. Our findings demonstrate the importance of studying the effects on T reg cells *in vivo* prior to the development of adjuvants.

Results

Systemic injection of Pam2 lipopeptides did not induce tumor growth retardation

To examine the anti-tumor effect of the Pam2 lipopeptides *in vivo*, mice were injected subcutaneously (s.c.) with NK-sensitive B16D8 melanomas into their back [22] and were treated with Pam2 lipopeptides twice a week (Fig. 1B). We selected four kinds of Pam2 lipopeptides, as shown in Fig. 1A, because they strongly activated NK cells through DCs and induced cytotoxic activity *in vitro* [25]. To our surprise, although the Pam2 lipopeptides activated NK cells *in vitro* [25], we did not observe effective anti-tumor response *in vivo* (Fig. 1B). To exclude the possibility that Pam2 lipopeptides were not distributed systemically, we investigated the activation of spleen DCs and NK cells by flow cytometry. The injection of Pam2 lipopeptides up-regulated CD86 and CD40 on splenic DCs (Fig. 1C). Similarly, CD69 was up-regulated in splenic NK cells (Supplemental Fig. S1). Thus, systemic injection of Pam2 lipopeptides was able to activate DCs and NK cells in the spleen, but did not induce effective anti-tumor responses *in vivo*.

Pam2 lipopeptides induce IL-10 *in vitro* and *in vivo* in a TLR2-dependent manner

To investigate why Pam2 lipopeptides could not induce effective anti-tumor responses against NK-sensitive tumors *in vivo*, we investigated whether Pam2 lipopeptides could activate suppressive factors, such as IL-10 and T reg -related molecules. For this experiment, we mainly used a representative Pam2 lipopeptide, Pam2CSK4, since Pam2CSK4 could activate DCs as well as other tested Pam2 lipopeptides *in vitro* [25].

When the mRNA levels from DCs stimulated with or without Pam2 lipopeptides were analyzed, Pam2 lipopeptides up-regulated retinal dehydrogenase 2 (RALDH2) and IL-10. RALDH2 in DCs activates retinoic acid, which is an important cofactor for TGF-b1 to induce Foxp3 [27,28]. However, Pam2 lipopeptides did not up-regulate the mRNA of TGF-b1 (Fig. 2A).

To confirm whether IL-10 protein is produced from DCs, we stimulated DCs with Pam2 lipopeptides *in vitro* for 24 hours and the concentration of IL-10 in the supernatants was measured by the ELISA. Bone-marrow derived DCs (BM-DCs) stimulated by Pam2 lipopeptides produced IL-10 (Fig. 2B). IL-10 was also produced by Pam2 lipopeptide-stimulated DCs from the spleen (data not shown). When DCs from TLR2- knockout (TLR2KO) mice were cultured with Pam2 lipopeptides, the production of IL-10 was not detected (Fig. 2B). Hence, IL-10 production was TLR2 dependent. Interestingly, we also found that Pam2 lipopeptides induced IL-10 production from NK cells (Fig. 2C).

To determine whether $CD4^+$ T cells produced IL-10 in the presence of Pam2 lipopeptides, OT II ovalbumin (OVA) transgenic $CD4^+$ T cells were cultured with DCs along with various doses of OVA peptide, with or without Pam2 lipopeptides (Fig. 2D). In the presence of Pam2 lipopeptides, more IL-10 was produced in the culture supernatants when OT II $CD4^+$ T cells were cultured with DCs and antigen (Fig. 2D). Importantly, IL-10 production was increased in an antigen-dose dependent manner (Fig. 2D).

Next, we analyzed the concentration of IL-10 in the serum of Pam2 lipopeptide-treated mice (Fig. 2E). When serum was taken at one day after Pam2CSK4 injection, significant amounts of IL-10 were detected (Fig. 2E), however, Th1, Th2 and Th17 cytokines were not detected (Fig. 2E). IL-10 production in serum was confirmed to be TLR2 dependent because we could not detect IL-10 in Pam2CSK4-treated TLR2KO mice (Fig. 2E). Taken together, these results indicated that Pam2 lipopeptides induce IL-10 both *in vitro* and *in vivo* in a TLR2-dependent manner, which might play a role in suppressing tumor immunity induced by Pam2 lipopeptides.

Systemic injection of Pam2 lipopeptides expands T reg cells through the TLR2 dependent production of IL-10

Since Pam2 lipopeptides induce IL-10, we investigated whether systemic injection of Pam2 lipopeptides could affect T reg cell frequencies. IL-10 produced by zymosan plays a role in inducing T reg cells [29]. We found that the frequency of $Foxp3^+$ T reg was increased in the spleen and lymph nodes at day 3 after systemic injection of Pam2CSK4 (Fig. 3A). The frequency of T reg cells had returned to normal by day 7 after Pam2CSK4 injection (Supplemental Fig. S2). The increase of T reg cells was dependent on TLR2 because T reg cells were not increased in TLR2KO mice injected with Pam2CSK4 (Fig. 3B).

To investigate whether the increase of $Foxp3^+$ T reg is dependent on the IL-10 produced by Pam2CSK4, mice were injected with neutralizing anti-IL-10 mAb (JES5-2A5) and Pam2CSK4 (Fig. 3C). Control mice injected with anti-IL-10 mAb alone or untreated mice were not included in this experiment, however, the frequency of $Foxp3^+$ T reg cells in the mice injected with anti-IL-10 Ab alone would be expected be similar to that of naïve mice since it is reported that the frequency of $Foxp3^+$ T reg cells is not affected in the spleen of IL-10 [30] or IL-10 receptor b knockout mice [31]. After three days, co-administration of anti-IL-10 mAb blocked the increase of T reg cells after Pam2CSK4 injection (Fig. 3C).

Therefore, Pam2 lipopeptides expand $Foxp3^+$ T reg cells at day 3 after systemic injection in a TLR2- and IL-10 dependent manner.

T reg cells from Pam2 lipopeptide-treated mice have suppressive activity

Next, we investigated the suppressive function of T reg cells in Pam2 lipopeptide-treated mice. We purified $CD25^+CD4^+$ T cells from naive mice or Pam2 lipopeptide-treated mice by flow cytometry (Fig. 4A). The frequency of $Foxp3^+CD4^+$ T cells in the purified $CD25^+CD4^+$ T cells from naïve mice or Pam2

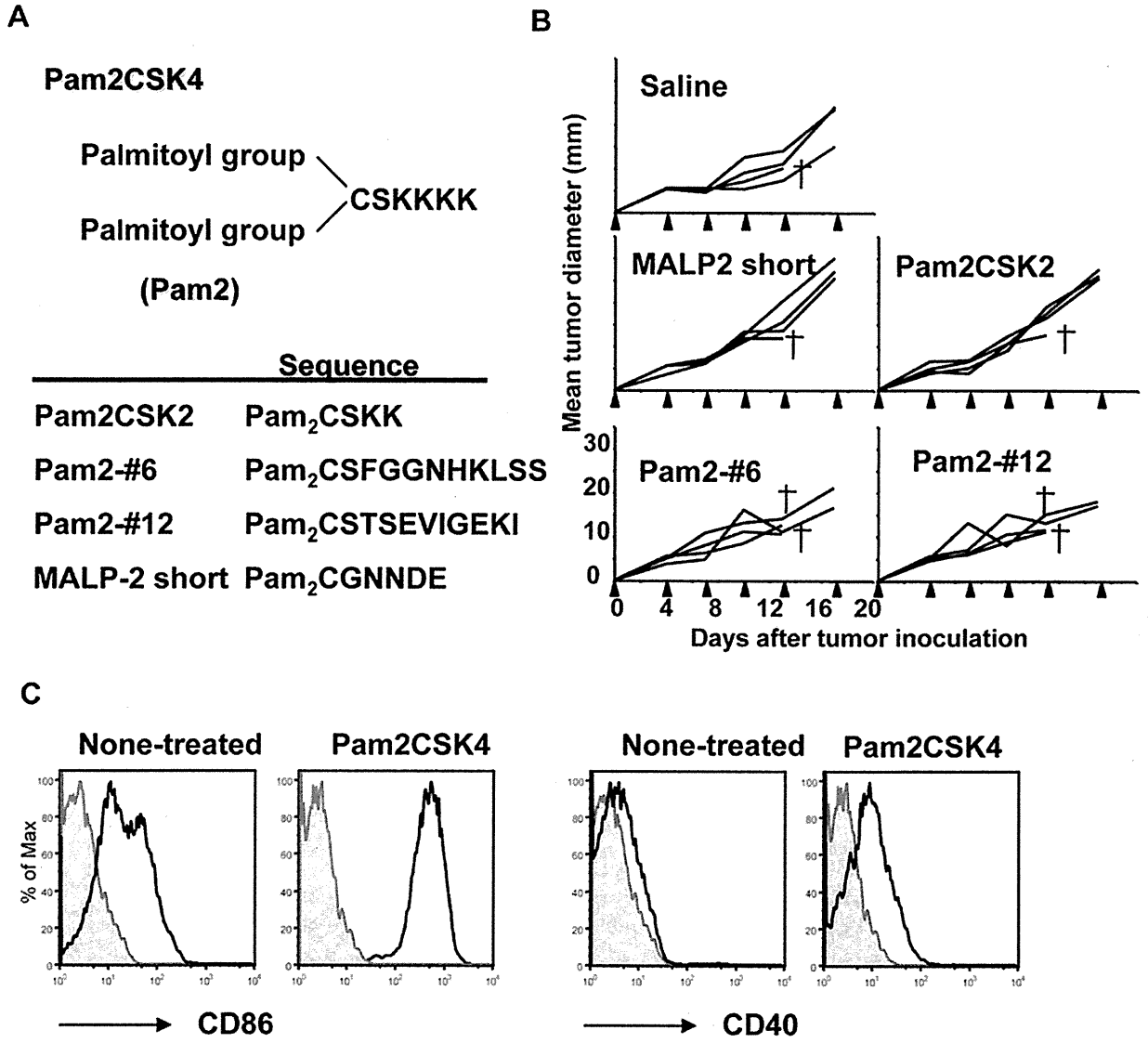

Figure 1. Pam2 lipopeptides do not induce effective anti-tumor immunity. (A) Structures of the Pam2 lipopeptides are shown. (B) Mice were injected with B16D8 melanoma cells (2×10^5) on back. The mice were injected s.c. into their footpad with the indicated Pam2 lipopeptides (10 nmol) or saline twice a week, as indicated by arrows, starting from day 0. Tumor growth was monitored in a blind manner. A cross indicates the death of one mouse. One of two experiments is shown. (C) Mice were injected with the indicated Pam2 lipopeptides (10 nmol) or saline. After 12–16 hours, spleen DCs were analyzed by flow cytometry. Plots were gated on $CD11c^+$ cells. One of two experiments is shown.
doi:10.1371/journal.pone.0018833.g001

lipopeptide-injected mice was always >95%, as shown in Fig. 4A. The purified $CD25^+CD4^+$ T cells were used for the classical *in vitro* suppression assay [32]. We found that the $CD25^+$ T reg cells from Pam2CSK4-treated mice suppressed the proliferation of $CD25^-$ $CD4^+$ T cells from naïve mice to a similar degree compared with the $CD25^+$ T reg from naïve mice (Fig. 4B, C). This indicated that Pam2 lipopeptides maintain T reg cell function *in vivo*.

Depletion of T reg cells improves the anti-tumor response by systemic injection of Pam2 lipopeptides

To determine whether systemic injection of Pam2 lipopeptides activates the function of T reg cells and suppresses anti-tumor responses against NK-sensitive tumors *in vivo*, we used an anti-CD25mAb (PC61) to deplete T reg cells *in vivo* before challenge with Pam2 lipopeptide and tumor cells [7–9]. Mice were injected with anti-CD25 mAb on day −3 and challenged with B16D8 melanoma cells on day 0, with or without Pam2CSK4 (Fig. 5A). As previously reported, depletion of T reg cells alone induced growth retardation of tumors [7–9]. Tumor growth was slightly promoted by Pam2CSK4 injection alone (Fig. 5A). However, the tumor growth in mice treated with anti-CD25 mAb plus Pam2CSK4 was slower than in mice treated with Pam2CSK4 alone (Fig. 5A, B). These results suggested that the presence of T reg cells suppressed effective anti-tumor responses after systemic injection of Pam2 lipopeptides.

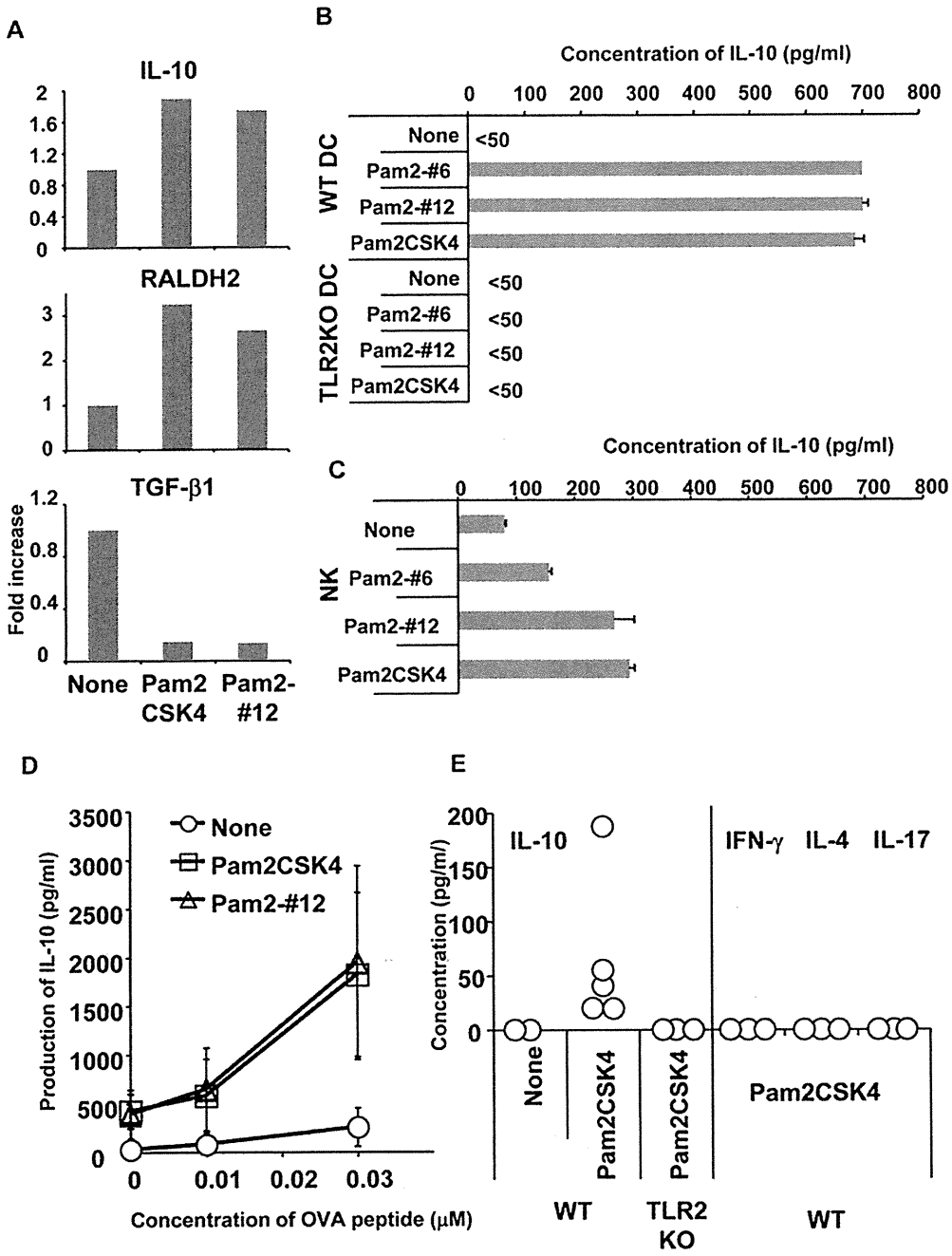

Figure 2. Pam2 lipopeptides induce IL-10 and retinal dehydrogenase. (A) Spleen DCs from B6 mice were cultured with or without 100 nM of Pam2CSK4 or Pam2-#12. After four hours, total RNA was prepared and real-time PCR was performed. Expression of each sample was normalized to GAPDH mRNA expression and fold increases of each sample were calculated to the expression levels at 0 hours. One of two experiments is shown. (B) BM-DCs (1×10^5) from wild type (WT) or TLR2KO mice were cultured with or without 100 nM of Pam2-#6, Pam2-#12 and Pam2CSK4 for 24 hours. The culture supernatants were measured for IL-10. One of two experiments is shown. (C) NK cells (2×10^5) from spleens were cultured with 100 nM of Pam2-#6, Pam2-#12 and Pam2CSK4 for 24 hours. The culture supernatants were measured for IL-10. One of two experiments is shown. (D) OT II $CD4^+$ T cells (5×10^4) were cultured with spleen DCs (5×10^4) with or without 100 nM of Pam2CSK4 or Pam2-#12 and the various doses of OVA peptide. After five days, supernatants were measured for IL-10. The means +/- SDs from two separate experiments is shown. (E) WT or TLR2KO mice were i.p. injected with 10 nmol Pam2CSK4 and next day serum was measured for the indicated cytokine concentrations.
doi:10.1371/journal.pone.0018833.g002

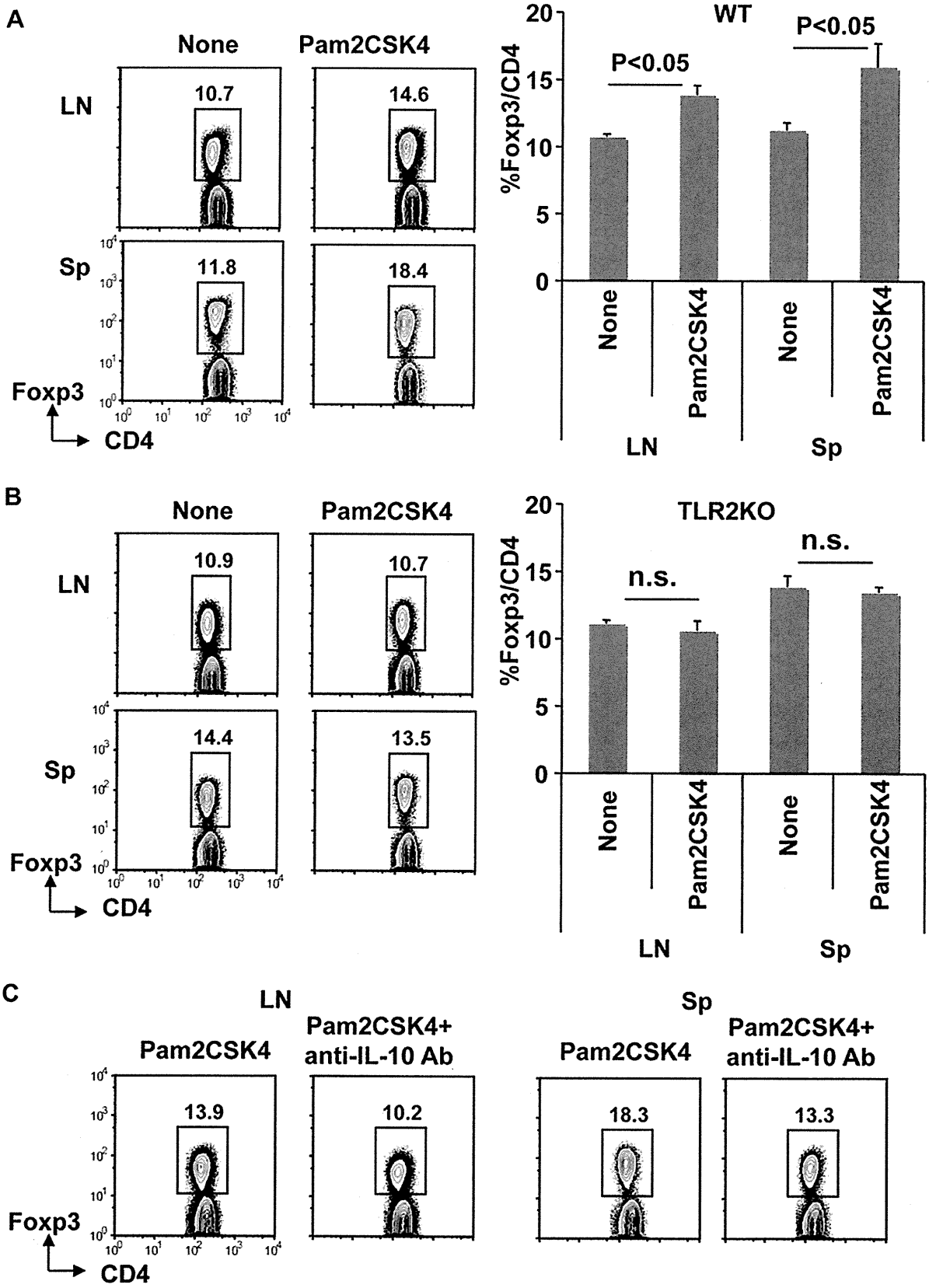
A
None
Pam2CSK4
LN
10.7
14.6
Sp
11.8
18.4
Foxp3
CD4
WT
P<0.05
P<0.05
%Foxp3/CD4
20
15
10
5
0
None
Pam2CSK4
None
Pam2CSK4
LN
Sp
B
None
Pam2CSK4
LN
10.9
10.7
Sp
14.4
13.5
Foxp3
CD4
TLR2KO
n.s.
n.s.
%Foxp3/CD4
20
15
10
5
0
None
Pam2CSK4
None
Pam2CSK4
LN
Sp
C
LN
Sp
Pam2CSK4
Pam2CSK4+
anti-IL-10 Ab
Pam2CSK4
Pam2CSK4+
anti-IL-10 Ab
13.9
10.2
18.3
13.3
Foxp3
CD4

Figure 3. Systemic injection of Pam2CSK4 expands Foxp3$^+$ T reg cells in a TLR2- and IL-10-dependent manner. (A) WT mice were i.p. injected with Pam2CSK4 (10 nmol). After three days, spleen (Sp) and lymph node (LN) cells were analyzed for the expression of Foxp3. The plots were gated on CD4$^+$ T cells. One of four experiments is shown for the FACS plots. The image summarizes the results of four separate experiments. P value is derived from the student's-t test. (B) As in (A), but TLR2KO mice were injected with Pam2CSK4. One of two experiments is shown for the FACS plots. The image summarizes the results from two separate experiments. N.s. stands for not significant according to the student's-t test. (C) As in (A), but mice were i.p. injected with Pam2CSK4 with or without 200 μg of anti-IL-10 mAb. One of two experiments is shown.
doi:10.1371/journal.pone.0018833.g003

Discussion

Here, we showed that systemic injection of Pam2 lipopeptides did not induce effective tumor immunity presumably because of the induction of IL-10 and T reg cells. To treat cancer, it is necessary to develop new adjuvants to activate immunity in immune-suppressed patients. Adjuvant activity is generally screened by analyzing its effect on effector cells such as NK cells and CD8$^+$ cytotocxic T cells. However, our results indicated that it is also important to investigate the activity of adjuvants on suppressive factors, such as IL-10 and T reg cells, particularly *in vivo*.

IL-10 is a key cytokine for IL-10 producing Tr1 regulatory T cells [33], and has also been shown to be an important cytokine for Foxp3$^+$ T reg cells. IL-10 production by Foxp3$^+$ T reg cells is required for the prevention of colitis [34,35]. The specific deletion of IL-10 in Foxp3$^+$ T reg cells in mice induces inflammation especially in the intestine, indicating that IL-10 derived from T reg cells plays a critical role in controlling colitis [35]. Furthermore, M. Kronenberg and his colleagues recently found that IL-10 secreted by other cells is needed for T reg cells to sustain expression of Foxp3 and prevent colitis [31]. This indicated that IL-10-enriched environments are preferable for Foxp3$^+$ T reg cells to exert their suppressive function *in vivo*. Here we have shown that systemic injection of Pam2 lipopeptides induces IL-10-rich environments *in vivo*, which could play a role in promoting T reg cell function.

Our results showed that TLR2-dependent production of IL-10 plays a role in expanding T reg cells *in vivo* (Fig. 3). This is consistent with a recent report by B. Pulendran and his colleagues who showed that TLR2 signaling by zymosan induces IL-10 and retinal dehydrogenase in DCs, which are critical for inducing T reg cells [29]. Zymosan binds to TLR2 and dectin-1 [29]. Our data showed that the TLR2 signal induced by Pam2 lipopeptides has a similar effect to the signal induced by zymosan. The TLR2 signal induced by zymosan results in the active suppression of experimental autoimmune encephalomyelitis (EAE) [29]. Furthermore, various TLR signals prevent the development of autoimmune type 1 diabetes in non-obese diabetic mice [36]. Our results showed that systemic injection of Pam2 lipopeptides was ineffective at inducing tumor immunity. However, it is possible that the Pam2 lipopeptides might be useful to inducing tolerance in the case of autoimmunity, allergy or transplant rejection.

In addition to the evidence that IL-10 produced in response to the TLR2 signal affects Foxp3$^+$ T reg cell function, the TLR2 signal can also directly act on T reg cells and promotes their survival [37]. Taken all together, although TLR2 activation by Pam2 lipopeptides is able to induce inflammatory cytokines and activate NK cells *in vitro* [25], the systemic injection of Pam2 lipopeptides as cancer adjuvants is ineffective at abolishing immune suppression. Whereas, the effective cancer adjuvant, BCG-CWS, activates not only TLR2, but also TLR4 and NOD2 receptors [23,38]. TLR2 activation by Pam2 lipopeptides could activate T reg cells *in vivo* and the T reg cells could suppress NK function and activation [39–41]. Our preliminary experiments showed that T reg cells actually suppress IFN-c production from NK cells stimulated with DCs plus Pam2CSK4 (S.Y., K.O., T.S., unpublished data). Here we showed that depletion of T reg cells with adjuvant might be one potential strategy to cancel the effect of activating suppressive factors by Pam2 lipopeptides.

We also found that Pam2 lipopeptides induce IL-10 production from NK cells *in vitro* (Fig. 2C). It has been known for over a decade that NK cells produce IL-10 [42–44]. Recent reports showed that IL-10 produced by NK cells play an important role in controlling T cell responses [45,46] and anti-inflammatory responses [47]. Moreover, IL-10 enhances the killing by NK cells of autologous antigen presenting cells [48,49]. These reports suggested that IL-10-stimulated NK cells could kill autologous macrophages and DCs, which may result in suppressing effective anti-tumor immunity. Therefore, it is possible that systemic injection of Pam2 lipopeptides in our system may induce IL-10 from NK cells and suppress anti-tumor response *in vivo*.

In contrast to the systemic injection of Pam2 lipopeptides, local injection of Pam2 lipopeptides was effective at suppressing tumor growth when the Pam2 lipopeptide was fused to RGDS-integrin peptides and injected around the tumor with tumor extracts [26]. This was probably effective for a few reasons:1) the peptide part of the Pam2 lipopeptide was fused with RGDS, which could promote the binding of Pam2 lipopeptides to DCs; 2) local injection of Pam2 lipopeptides around the tumor may be different from systemic injection of Pam2 lipopeptides in terms of inducing IL-10 and T reg cells. Other literature has also indicated that local administration of Pam2 lipopeptides could be effective for cancer [50,51]. The differential effect on inducing IL-10 and T reg cells between local administration and systemic injection of adjuvants should be investigated further in future studies.

The literature on TLR2 signaling and T reg cells is controversial. Some groups reported that T reg cells temporally lost their suppressive capacity in the presence of the TLR2/TLR1 ligand Pam3CSK4, which contains 3-palmitoyl bases [52,53]. However, a recent report from E. Shevach and his colleagues showed that the presence of Pam3CSK4 in the culture actually maintained the suppressive function of T reg cells and promoted their survival [37]. This discrepancy might be caused by the use of CD25$^+$ CD4$^+$ T cells contaminated with Foxp3$^-$CD25$^+$CD4$^+$ T cells, and Foxp3-GFP reporter mice [37]. Contamination of Foxp3$^-$CD25$^+$CD4$^+$ T cells could affect the results, especially when TLR2 ligands were continuously present in the culture, since TLR2 is also expressed on activated effector T cells. In this report, we stimulated T reg cells with Pam2 lipopeptides *in vivo* and purified T reg cells as CD25$^+$ CD4$^+$ T cells because Foxp3-GFP reporter mice were not available. However, CD25$^+$ CD4$^+$ T reg cells purified from Pam2CSK4 treated mice were as suppressive as T reg cells from naïve mice (Fig. 4B). This indicated that T reg cells stimulated by TLR2 did not reverse the suppressive function *in vivo*.

To fight to cancer, it is very important to develop an adjuvant to activate immunity. However, it is also crucial to consider the effect of adjuvants on suppressive factors such as IL-10 and T reg cells. The combination of adjuvant and blockade of IL-10 or T reg cell function might prove a successful strategy for improving cancer vaccines.

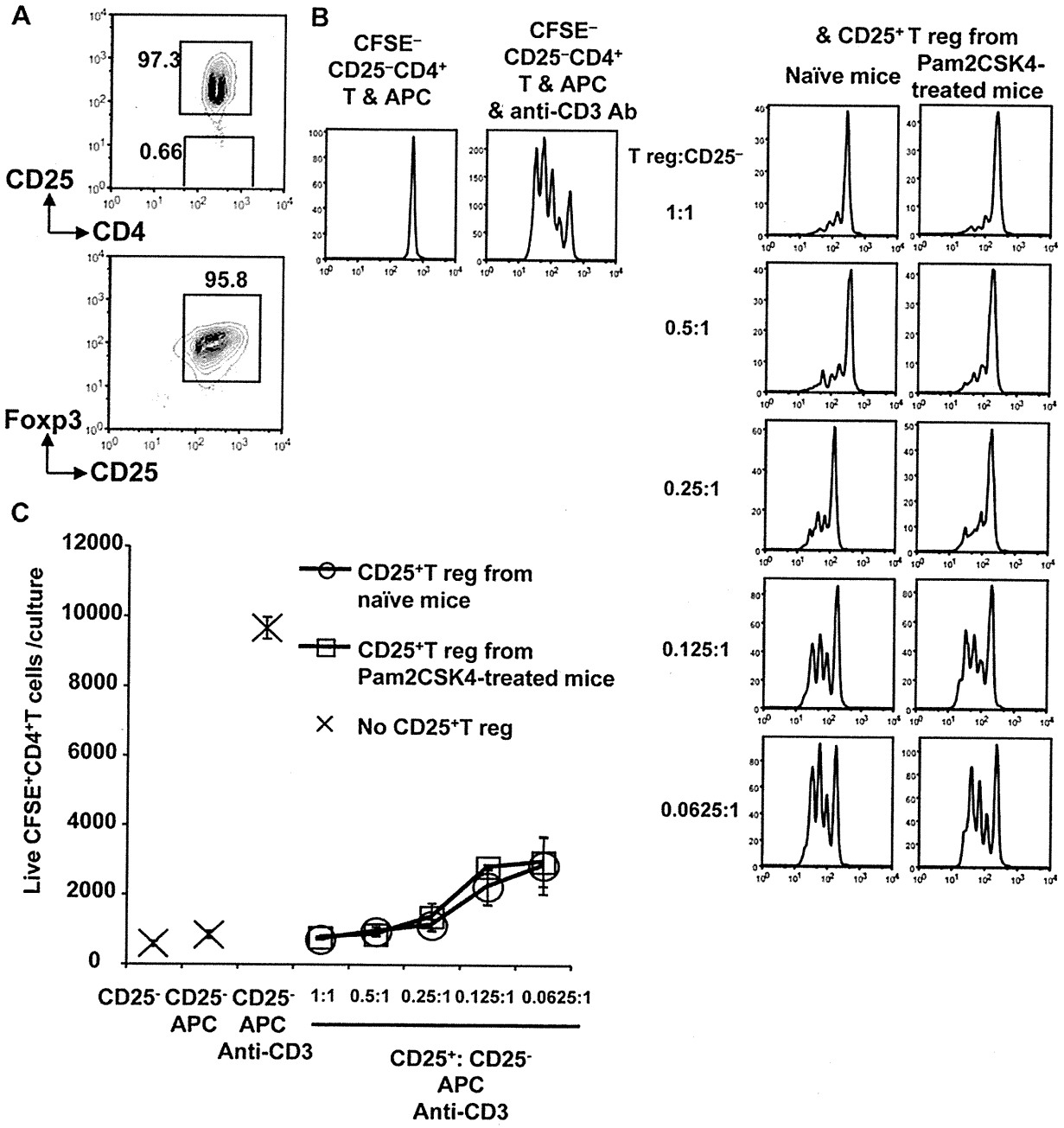

Figure 4. T reg cells from Pam2CSK4-treated mice maintain suppressive activity. (A)$CD25^+CD4^+$ T cells purified by flow cytometry were further fixed and stained with Foxp3. FACS plots were gated on $CD4^+$ T cells. One of three similar experiments is shown.(B) B6 mice were i.p. injected with Pam2CSK4 (10 nmol) on days 0, 3 and 7. On day 14, $CD25^+CD4^+$ T cells purified as in (A) were used for the suppression assay. CFSE-labeled $CD25^-$ $CD4^+$ T cells (5×10^4) were stimulated with irradiated spleen antigen presenting cells (1×10^5) with or without 5% anti-CD3 mAb supernatant. The purified $CD25^+CD4^+$ T cells from naïve mice or Pam2CSK4-treated mice were added at the indicated ratio. After three days, cells were stained with CD4 and analyzed with CFSE dilution. Dead cells were eliminated by TOPRO-3. One of three similar experiments is shown. (C) As in (B), but the numbers of live $CFSE^+$ $CD4^+$T cells per culture were plotted. One of three similar experiments is shown.
doi:10.1371/journal.pone.0018833.g004

Materials and Methods

Mice

C57BL6J (B6) mice and CB17SCID mice were obtained from Japan Clea (Tokyo, Japan). TLR2KO mice were provided by Dr. Shizuo Akira (Osaka University, Osaka, Japan). OT II OVA CD4 transgenic mice were kindly provided from Dr. Kazuya Iwabuchi (Kitasato University, Kanagawa, Japan). The mice were maintained in the Hokkaido University Animal Facility (Sapporo, Japan) in specific pathogen free condition. All